Performance Analysis of Transmit Diversity STBC-OFDM and Differential STBC-OFDM Over Fading Channels

Emad M. Mohamed

Submitted to the
Institute of Graduate Studies and Research
in partial fulfillment of the requirements for the Degree of

Master of Science
in
Electrical and Electronic Engineering

Eastern Mediterranean University
May 2013
Gazimağusa, North Cyprus

Approval of the Institute of Graduate Studies and Research

Prof. Dr. Elvan Yılmaz
Director

I certify that this thesis satisfies the requirements as a thesis for the degree of Master of Science in Electrical and Electronic Engineering.

Prof. Dr. Aykut Hocanın
Chair, Department of Electrical and Electronic Engineering

We certify that we have read this thesis and that in our opinion it is fully adequate in scope and quality as a thesis for the degree of Master of Science in Electrical and Electronic Engineering.

Assoc. Prof. Dr. Erhan A. İnce
Supervisor

Examining Committee

1. Prof. Dr. Şener Uysal
2. Assoc. Prof. Dr. Hasan Demirel
3. Assoc. Prof. Dr. Erhan A. İnce

ABSTRACT

Alamouti space-time block coding (A-STBC) is a relatively well known coding technique that is employed to enhance the capacity of wireless communication systems without affecting the bandwidth efficiency. Furthermore, A-STBC is known to have a linear decoding complexity which has made it one of the most popular among space time codes (STCs). The decoding of space-time block codes, however, requires knowledge of channel state information (CSI) at the receiver and in general, channel parameters are assumed to be known (assumes that channel estimation is possible). However, when there is high mobility and the channel conditions are fluctuating rapidly it may be difficult to obtain perfect or close to perfect estimates for the channel. To alleviate this problem another space-time block coding technique known as Differential Space-Time Block Coding (DSTBC) has been proposed. Differential phase shift keying (DPSK) which is employed by DSTBCs is a common form of phase modulation that conveys data by changing the phase of the carrier wave. The decoder in DPSK modulation does not require CSI since the transmitted symbols depend on the previous symbol and the decoder would sense the data from symbols that come one after another. When channel fluctuations are very high DSTBCs need to be used at the expense of lower bit error rate.

The work presented herein, provides a link level bit error rate analysis of none line-of-sight (NLOS) Alamouti space-time block coded with Orthogonal Frequency Division Multiplexing (OFDM) using either BPSK or QPSK modulation. OFDM is a multicarrier modulation technique where a high rate data stream is sub-divided

into a number of lower rate data streams and transmitted over a number of subcarriers. The performance increment due to OFDM comes from the fact that the usage of a guard interval that help reduce or completely eliminate the interference between symbols due to multipath effect.

The simulation results presented in this thesis have all been obtained using the readily available MATLAB platform and writing dedicated functions for different tasks. The results have been presented in four parts. The first part provides the bit error rate performance for BPSK modulated data transmitted over a Rayleigh fading channel. This is then followed by a performance analysis of OFDM over the AWGN channel using either BPSK or QPSK modulation. Third part demonstrates the BER vs. SNR for Alamouti STBC and Alamouti DSTBC coded data transmitted over a Rayleigh fading channel without using OFDM. Finally, part four will provide STBC and DSTBC coded OFDM performance when BPSK and QPSK are the preferred modulation and the channel is again the Rayleigh fading channel.

The work presented clearly demonstrates that even though OFDM by itself is giving good performance by mitigating inter-symbol interference, combining OFDM with a transmit diversity technique like Alamouti STBC helps further improve the link level BER performance. The simulation results indicate that when no CSI is available and DSTBC needs to be employed, the system performance will degrade approximately by 2.2dB at a BER of 10^{-4} (in comparison to STBC-OFDM using BPSK).

Keywords: STBC, DSTBC, OFDM, Rayleigh Fading, BER.

ÖZ

Alamouti uzay-zaman blok kodlama yöntemi (A-UZBK) nispeten iyi tanınan ve bant genişliği verimini etkilemeksizin kablosuz iletişim kapasitesini artırmak üzere yararlanılan bir yöntemdir. Buna ek olarak A-UZBK çözücüsünün doğrusal bir kod çözme karışıklığına sahip oluşu da bu yöntemi diğer uzay-zaman kodlayıcılar arasında öne çıkarmaktadır. Genellikle Alamouti uzay-zaman blok kodlama tekniğinin kod çözücüsü kanal durum bilgilerinin (KDB) bilinmesini gerektirmektedir ki bu da kanal tahmininin mümkün olduğu varsayımını gerektirir. Fakat yüksek hareketlilik oranının bulunduğu ve kanal koşullarının hızlı bir dalgalanma gösterdikleri durumlarda kanal için mükemmel veya mükemmele yakın tahminlerin elde edilmesi zorlaşabilmektedir. Bu problemin hafifletilmesi için Fark-Kodlamalı Uzay-Zaman Blok Kodlama (FK-UZBK) yöntemi önerilmiştir.

FK-UZBK'lar tarafından kullanılan diferansiyel faz değiştirme anahtarlama (DPSK) yöntemi, taşıyıcı dalganın fazını değiştirerek verileri ileten yaygın bir faz geçiş şeklidir. İletilen semböller bir önceki semböle bağlı olup şifre çözücü verileri birbiri ardına gelen semböllerden algıladığından DPSK modülasyondaki şifre çözücü KDB'ni gerektirmemektedir. Kanal dalgalanmalarının yüksek olduğu durumlarda FK-UZBK'ların daha düşük bit hata oranı pahasına kullanılması bir zorunluluk olmaktadır. Bu çalışmada, Alamouti uzay-zaman blok kodlarıyla ikili ve dörtlü faz kaydırmalı kipleme kullanan Dikgen Frekans Bölüşümlü Çoğullama (DFBÇ) yöntemi birleştirilerek görüş hattı dışındaki (NLOS) durumlar için link seviyesinde bit hata oranı analizi gerçekleştirilmiştir.

DFBÇ, yüksek hızlı veri akışına sahip bir katarın daha düşük hızlardaki birden fazla katara bölündüğü ve birçok alt taşıyıcı üzerinden aktarma yapılan çoklu taşıyıcılı bir modülasyon tekniğidir. DFBÇ'deki performans artışı, çoklu yol etkisinden kaynaklanan semböller arası karışmaların azaltılması veya tamamen ortadan kaldırılmasına yardımcı olan bir koruma bandının (çevrimsel öntakı) kullanımı ile sağlanmaktadır. Bu tez çalışmasında sunulan tüm benzetim sonuçları MATLAB platformunu kullanarak ve gerekli tüm görevler için adanmış fonksiyonlar yazarak elde edilmiştir. Sonuçlar dört bölüm halinde sunulmuştur. İlk bölüm, ikili faz kaydırmalı kiplenmiş verinin bir Rayleigh kanalı üzerinde göndrildiği durumlardaki bit hata oranı verimini sunmaktadır.

Daha sonra ikinci bölümde ikili ve dörtlü faz kaydırmalı kipleme kullanan DFBÇ'nin Toplanır Beyaz Gauss Gürültü (TBGG) kanal üzerindeki performansı incelenmiştir. Üçüncü bölümde DFBÇ kullanılmadan yavaş sönümlemeli bir Rayleigh kanalı üzerinden aktarılan Alamouti UZBK ve Alamouti FK-UZBK ile kodlanmış veriler için bit-hata-oranı karşılaştırma sonuçları sunulmaktadır. Son olarak dördüncü bölüm ikili ve dörtlü faz kaydırmalı kipleme tekniklerinin tercih edildiği ve kanalın yine yavaş sönümlemeli bir Rayleigh kanalı olduğu durumlar için A-UZBK ve Alamouti FK-UZBK yöntemleri ile kodlanmış DFBÇ için elde edilen bit-hata-oranlarını sunmuştur.

Yapılan çalışmalarda görülmüştür ki her ne kadar da DFBÇ semböller arası karışmaları hafifleterek tek başına iyi bir performans gösterse de, DFBÇ'nin Alamouti UZBK gibi bir gönderim çeşitleme tekniği ile birleşiminden elde edilecek bağlantı düzeyi bit-hata-oranları daha da iy olmaktadır. Simülasyon sonuçları

KDB'nin mevcut olmadığı ve FK-UZBK'nin kullanımının gerekli olduğu durumlarda sistem performansının 10^{-4} bit-hata-oranında yaklaşık olarak 2.2 dB gerilediğini göstermiştir (ikili faz kaydırmalı kipleme kullanan UZBK-DFBÇ ile karşılaştırıldığında).

Anahtar Kelimeler: UZBK, Diferansiyel UZBK, DFBÇ, Çoklu-Çıkış, Rayleigh Zayıflama.

ACKNOWLEDGMENTS

I would like to thank Assoc. Prof. Dr. Erhan A. İnce for his continuous support and guidance in the preparation of this study. Without his invaluable supervision, all my efforts could have been short-sighted.

I also would like to thank the Chairman, Prof. Dr. Aykut Hocanın and all academic staff and personnel at the Electrical and Electronics Engineering department for providing their help and support during my course of study at Eastern Mediterranean University.

Besides, a number of friends had always been around to support me morally. I would like to thank them as well.

I owe a lot to my family who allowed me to travel for the purpose of study and supported me during my studies. I would like to dedicate this thesis to them as a sign of gratitude to them.

TABLE OF CONTENTS

LIST OF TABLES

LIST OF FIGURES

LIST OF SYM BOLS AND ABBREVIATIONS

B	Transmission bandwidth (hertz)
B_c	Coherence bandwidth
B_s	Coherence bandwidth
C	Channel capacity (bits/s)
$\frac{E_b}{N_0}$	Energy per bit to noise power spectral density ratio
$\frac{E_s}{N_0}$	Energy per symbol to noise power spectral density ratio
f_c	Carrier frequency
f_d	Doppler frequency associated with Rayleigh fading channels
f_m	Maximum Doppler frequency
R_x	Receiver
T_c	Coherence time
T_x	Transmitter
σ^2	Channel noise variance
σ_τ	Root mean square delay spread
η_t	Zero mean additive white Gaussian noise
θ	Phase of the multipath component
3G	Third generation

4G	Fourth Generation
3GPP	3^{th} Generation Partnership Project
AWGN	Additive white Gaussian noise
BS	Base Station
BER	Bit error rate.
BPSK	binary phase shift keying
bps	Bit per second
CC	Convolutional Code
CSI	Channel state information
CP	Cyclic prefix
DPSK	Differential phase shift keying
DSTBC	Differential Space Time Block Coding
FEC	forward error correction
FFT	Fast Fourier Transform
ICI	Inter Carrier Interference
IFFT	Inverse Fourier Transform
ISI	Inter Symbol Interference
LDPC	Low Density Parity Check Code
LOS	Line of Sight
MCM	Multi-carrier modulation

MIMO	multiple-input multiple-output
MISO	Multiple-input single-output
ML	Maximum likelihood
MLD	Maximum likelihood Detector
MLSE	Maximum likelihood sequence estimation
MS	Mobile station
NLOS	Non Line of Sight
OFDM	Orthogonal Frequency Division Multiplexing
OFDMA	Orthogonal Frequency Division Multiple Access
PSK	Phase-Shift Keying
QPSK	Quadrature Phase-Shift Keying
RMS	root mean square
SISO	Single Input Single Output
SNR	Signal to Noise Ratio
STBC	Space Time Block Coding
STC	Space Time Coding
TC	Turbo Coding
TD	transmit diversity

Chapter 1

INTRODUCTION

High data rate, spectrum efficiency, coverage and link reliability are the main issues that many wireless design engineers are constantly trying to improve. In this thesis Multiple Input Multiple Output (MIMO) systems employing transmit diversity combined with Orthogonal Frequency Division Multiplexing (OFDM) technique is studied and the systems bit error rate (BER) performance is analyzed over a flat Rayleigh fading channel for conventional Space Time Block Coding (STBC) and differential STBC (DSTBC).

1.1 Background

Since multipath environments can cause severe degradation while a data are being transmitted on the communication channel, deployment of MIMO systems has helped enhance channel capacity and improve link level reliability by making use of spatial diversity. In [1] it is stated that the first bandwidth efficient transmit diversity scheme had been proposed by Wittneben [2] where the authors make use of a special case of delay diversity proposed by Seshadri and Winters [3]. More recently space-time trellis coding has been proposed in [4] by Tarokh Seshadri and Calderbank. For slow fading environments such as indoor transmission, space-time trellis codes with two or four transmit antennas are known to give good performance. In fact their BER performance would approach 2-3dB of the outage capacity computed by Telatar in [5]. When the number of transmit antennas is fixed, the decoding complexity of space-time trellis coding would be increasing exponentially (measured in number of trellis states at decoder) as a function of diversity and transmission rate.

While addressing the decoding complexity the very first breakthrough has come with Siavash M. Alamouti. As explained in [6], Alamouti had proposed a new space-time block coding technique utilizing a two-branch transmit diversity to code and transmit the data over two independent channels. Furthermore, it was shown that either using the simple Alamouti decoder [7] or the Maximum Likelihood (ML) [8] decoder the received copies of the noisy signals can be easily combined and decoded. The decoding complexity of the Alamouti decoder has been demonstrated to be linear. A comparative analysis of computational complexity of detection methods have been provided in [9] for the interested reader.

The transmission scheme proposed by Alamouti (2×1 transmit diversity) was later generalized by [10] and [11] so that an arbitrary number of transmitting antennas can be employed and yet full diversity can be achieved. Most studies in the literature [12-14] assume that the channel state information is known to the receiver. However in practice, for fast fading channels this may not always be possible and requires use of non-coherent detection techniques. Tarokh and Jafarkhani [15], were the first to propose a detection mechanism for non-coherent scenario (making use of differential detection). Other authors like Kim [16] and Abdalla [17] later also presented results using differential STBC (DSTBC) and MIMO-OFDM.

For broadband scenarios most of the time the communication channel is time-varying and hence the frequency selective. In order to deal with such severe multipath propagation environments a combination of MIMO coding techniques with OFDM is required. In fact MIMO-OFDM has already been adopted by third and fourth generation future broadband communication standards such as Long Term Evolution (LTE) [18] in 3GPP and 3GPP2 projects and IEEE 802.16d and IEEE 802.16e standards for Worldwide Interoperability for Microwave Access (WiMax) [19]. In [20], Suraweera suggested that an auto regressive (AR) model is used to model the time-selectivity of a typical Rayleigh fading channel. For time selective channels the correlation coefficient would be equal to $J_{0\,(2\pi f_d T_s)}$ where $J_{0\,(.)}$ is the 0^{th} order Bessel function, f_d is the maximum Doppler spread and T_s is the OFDM symbol duration [21].

The basic idea behind OFDM is to break a high data rate stream into multiple parallel streams with lower rates and hence turn the wideband channel into multiple narrowband channels. Use of slowly modulated multiple signals has the following advantages. The low symbol rate makes usage of guard interval affordable and also the channel equalization becomes simpler.

The scarceness of the available spectrum brings the need for using the available bandwidth efficiently and interference due to multipath and other users requires counter measures to improve the link reliability. To achieve both of these 4G mobile wireless communication systems prefer to combine MIMO and OFDM techniques. OFDM which is known to mitigate the severe fading effect of wideband channels when combined with MIMO systems can also improve on link reliability by using antenna diversity gain.

The goal of this thesis is to highlight the advantages of combining MIMO and OFDM techniques when either the conventional Alamouti transmit diversity or differential STBC is employed to transmit BPSK or QPSK modulated symbols. The organization of the thesis is discussed in the section that follows.

1.2 Thesis Outline

The contents of this thesis is organized as follows. Following a general introduction, the background survey and the description on how the thesis has been organized in Chapter1, Chapter 2 provides description of the channel models: namely AWGN and flat Rayleigh fading channels. Chapter 2 also provides explanations about the important channel parameters: rms delay spread, maximum excess delay, coherence bandwidth, coherence time and Doppler spread. The Orthogonal Frequency Division Multiplexing (OFDM) technique which is used to convert a wideband channel into multiple narrowband channels is introduced in Chapter 3. This chapter first gives a description of the various blocks in an OFDM system and explains the need for using a Cyclic Prefix (CP). It also provides an equation for SNR loss due to the use of a CP and concludes by providing an equation for transmission efficiency. MIMO techniques with transmit diversity making use of STBC is introduced in Chapter 4. Particularly Alamouti STBC and Alamouti DSTBC are explained in detail. In Chapter 5 simulation results on link-level BER performance will be provided for both STBC-OFDM and DSTBC-OFDM using BPSK and QPSK modulation. Finally, Chapter 6 will provide the conclusions for the thesis.

Chapter 2

CHANNEL MODELS

The propagation of radio waves through the atmosphere including the ionosphere is not a simple phenomenon to model. Atmospheric propagation can show a wide range of behaviors based on factors like frequency, bandwidth of the signal, types of antennas used, terrain and weather conditions. When there is no fading, the channel can be assumed to be additive. If the samples are independent of each other the additive noise is referred to as 'white' and then they are correlated are referred to as 'colored'. The simplest communication channel model is the Additive White Gaussian Noise model under which the signal is affected only by a constant attenuation. In wireless communication channels there will be more than one path in which the signal can travel between the source and destination. The presence of these paths is due to atmospheric reflections, refractions and scattering. In a multipath fading environment if a line of sight (LOS) component is available then the channel is referred to as a Rician channel. On the other hand if there is no LOS component then the channel will be referred to as a Rayleigh fading channel.

2.1 AWGN Channel

A channel is defined as a single path for transmitting either in one direction or two (duplex mode). Wireless channel modeling is carried out to come up with applicable analytical models that reflect the changes in the communication channel. In all communication channels there is a common part which is the additive noise. When the noise samples are independent of each other this noise is called Additive White Gaussian Noise (AWGN) [22]. AWGN noise can be expressed as the linear addition of wideband or white noise that has a flat (constant) spectral density. The amplitude of the noise samples has a Gaussian distribution. AWGN in general do not account for fading, frequency selectivity or dispersion. A general block diagram for the AWGN channel has been depicted in Figure 2.1.

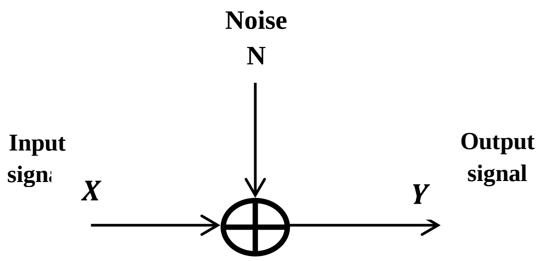

Figure 2.1 : AWGN Channel Model

The effect of the AWGN channel on a signal can be expressed as, $\boldsymbol{Y} = \boldsymbol{X} + \boldsymbol{N}$, where $\boldsymbol{N}$ is the additive Gaussian noise, $\boldsymbol{X}$ and $\boldsymbol{Y}$ are respectively the input and the output of the channel. The statistical model for the AWGN channel with zero mean can be shown by the probability density function (pdf) in (2.1) [23]:

$$p(x) = \frac{1}{\sqrt{2\pi\sigma^2}} exp\left(\frac{-x^2}{2\sigma^2}\right) \qquad (2.1\ )$$

Where,σ^2represents the variance of the noise.

The source of Gaussian noise may come from many natural sources. Some examples include thermal vibrations of atoms, black body radiation and shot nois. The capacity of an AWGN channel has been derived from Shannon Claude and is as follows:

$$C = Blog_2\left(1 + \frac{P}{N_0 B}\right) \tag{2.2}$$

where, B is the transmission bandwidth in Hz , P is the received signal power in Watts and N_0 is the single sided noise power spectral density in Watts/Hertz.

2.2 Fading Channel

In wireless channels, signal fading is caused mainly by multi-path propagation. The presence of multi-path is either due to atmospheric reflections/refractions or reflections/scattering from buildings, trees and geographical structures. Multi-path implies that many copies of the transmitted signal will reach the receiver and each copy will have a different amplitude and delay. Sometimes the received copies of the signals will add constructively and at other times destructively. When they add destructively this will cause deep fades in the frequency response of the channel and cause severe attenuation of the transmitted signal. Figure 2.2 depicts the possible causes of multi-path propagation between a base station and mobile subscribers.

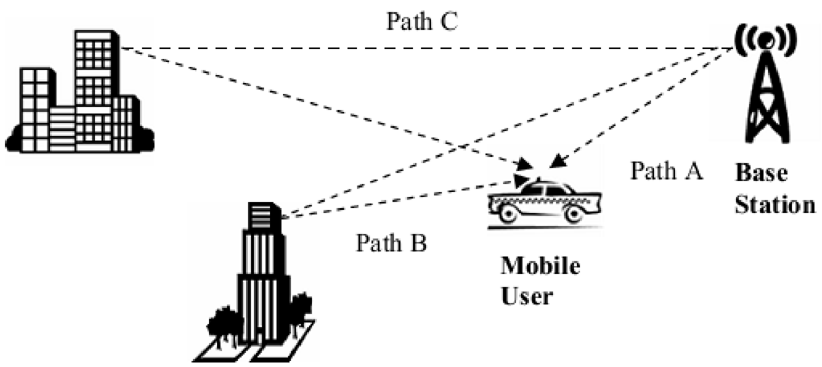

Figure 2.2 : Wireless Fading Channel and Multi-Path Propagation [24].

Radio signals propagating in an environment with obstacles will be affected in three different ways. The signal may be attenuated, get exposed to shadowing and/or small-scale fading. If there are multiple reflective paths, and there is no line-of-sight (NLOS) signal component then the channel is classified as a Rayleigh fading channel [24]. In the statistical modeling of the Rayleigh fading channel a normalized Rayleigh distribution with given mean and variance is used.

$$p(a) = \begin{cases} 2a\, exp(-a^2) & , a \geq 0 \\ 0 & a < 0 \end{cases} \tag{2.3}$$

$$m_a = 0.8862 \tag{2.4}$$

$$\sigma_a^2 = 0.2146 \tag{2.5}$$

Where, a represents the random variates, m_a denotes the mean and σ_a^2 is the variance.

2.3 Parameters of the Mobile Multipath Channel

The power delay profile (PDP) gives the intensity of a signal received through a multipath channel as a function of time delay. The parameters of the mobile multipath channel are some brief descriptions

2.3.1 Maximum Excess Delay

Maximum excess delay is the time delay during which multipath power falls to (S dB) below the maximum. Hence, the maximum excess delay can be defined as $t_s - t_0$ where t_s is the maximum delay and t_0 is the time of the first received signal at which a multipath component is within (S dB) of the strongest received multipath signal [25]. Figure 2.3 depicts the calculation of the maximum excess delay for a multipath channel.

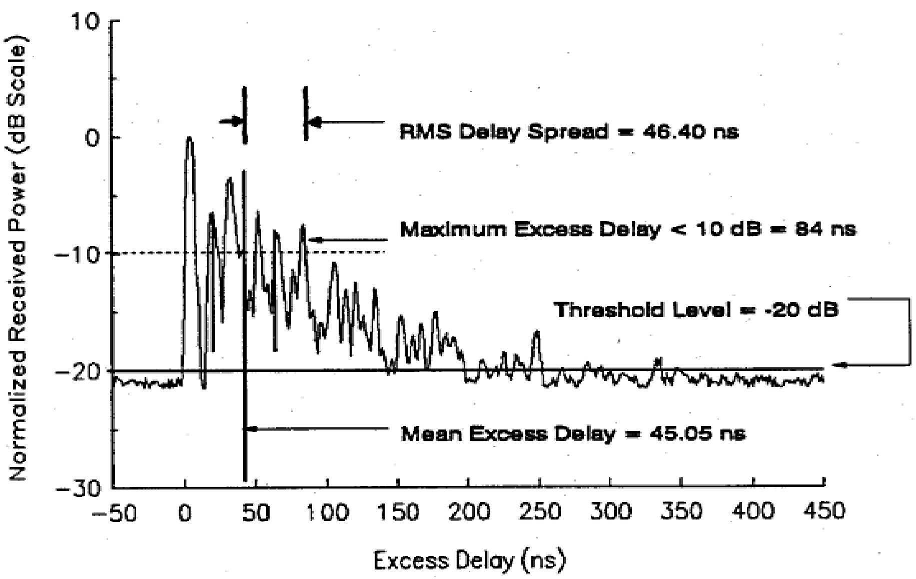

Figure 2.3: Power Delay Profile for a Wireless Channel [25].

2.3.2 Root Mean Square Delay Spread

RMS delay spread which is based on mean excess delay, is defined as the square root of the second moment of the power delay profile and as described in [26] can be written as:

$$\sigma_\tau = \sqrt{\overline{\tau^2} - \bar{\tau}^2} \tag{2.6}$$

$$\overline{\tau^2} = \frac{\sum_k P(\tau_k)\tau_k^2}{\sum_k P(\tau_k)} = \frac{\sum_k a_k^2 \tau_k^2}{\sum_k a_k^2} \tag{2.7}$$

$$\bar{\tau} = \frac{\sum_k a_k^2 \tau_k}{\sum_k a_k^2} \tag{2.8}$$

Here $\bar{\tau}$ is the mean excess delay and $\overline{\tau^2}$ is the mean of the squared excess delay [25]. Points out that, for outdoor channels typical values for *rms* delay spread is on the order of microseconds.

2.3.3 Coherence Bandwidth

Coherence bandwidth B_c of a radio channel is a statistical measure of the range of frequencies over which the channel can be considered "flat" (i.e, channel passes all spectral components with equal gain). Based on the degree of correlation that may exist different approximations for B_c are possible. For frequency correlation function above 0.9 the coherence bandwidth is as defined in [26]:

$$B_c \approx \frac{1}{50\sigma_\tau} \tag{2.9}$$

And when frequency correlation function is above 0.5, coherence bandwidth and the rms delay spread can be roughly related as:

$$B_c \approx \frac{1}{5\sigma_\tau} \tag{2.10}$$

2.3.4 Doppler Spread and Coherence Time

Doppler spread is defined as the frequency shift that occurs in a wireless communication channel due to the relative motion of the receiver as in the case of a mobile unit. The amount of shift is proportional to the speed of the mobile and the angle of incidence (θ). We can define the shift in the carrier frequency due to Doppler as:

$$f_d = \frac{v \cdot f_c}{c} \cos\theta \tag{2.11}$$

Where, v is the speed of the mobile in meters, c is the speed of light, f_c is the carrier frequency and θ represents the angle of incidence. The effect of the spread in frequency is usually inter-symbol-interference (ISI), an undesired degrading effect.

Doppler spread experienced in a wireless channel is inversely proportional to the coherence time T_c of the channel [25].

Coherence time is the time-domain dual of the Doppler spread and is used for describing the frequency depressiveness of the channel in the time-domain. An approximation for the coherence bandwidth is:

$$T_c \approx \frac{1}{f_m} \tag{2.12}$$

Where, f_m denotes the maximum Doppler shift and equals:

$$f_m \approx v/\lambda \tag{2.13}$$

2.4 Small Scale Multipath Propagation

Multipath in radio channels is the main cause for small-scale fading in the communication medium. Small scale fading or short time fading is the name given to changes in amplitudes, phases and delays of signals over a short period of time. Rapid changes in signal strength, random frequency modulations due to variations in Doppler shift and time dispersions (echoes) are all caused by small-scale multipath propagation. Figure 2.4 shows two different types of small scale fading due to multipath. These are mainly called flat fading and frequency selective fading.

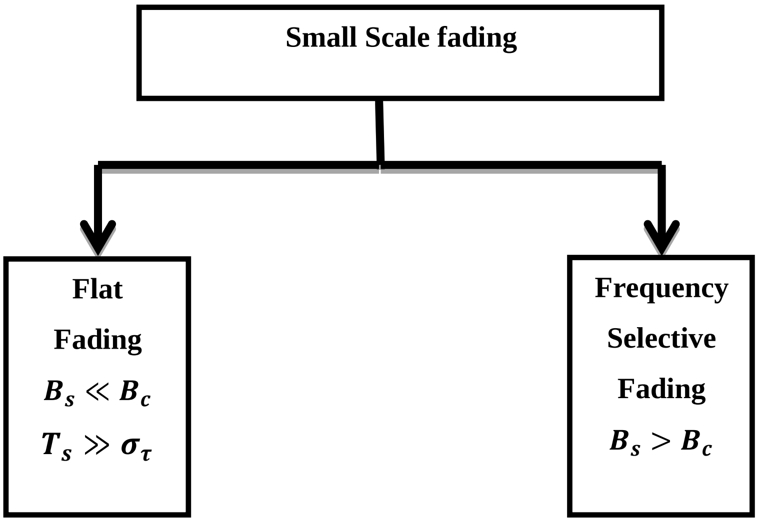

Figure 2.4: Types of Small-Scale Fading.

2.4.1 Flat Fading

Flat fading channels are often referred to as narrowband channels. When the bandwidth of the signal (B_s) to transmit is much smaller than the coherence bandwidth of the channel it will be transmitted over then the channel is referred to as flat fading channel. The effect of the flat fading on the transmitted signal has a single pulse is depicted in Figure 2.5 in time and frequency domains.

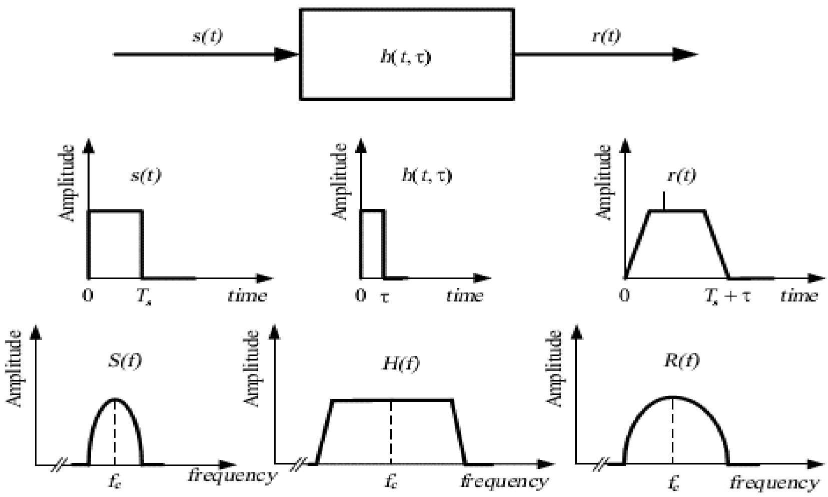

Figure 2.5: Pulse and Frequency Response Shaping by a Flat Fading Channel [25].

2.4.2 Frequency Selective Fading

As depicted in Figure 2.6, the coherence bandwidth B_c of a frequency selective fading channels is smaller than that of a transmitted signal's bandwidth B_s. In frequency domain, the channel becomes frequency selective, where the gain is variation for different frequency components. Frequency selective fading is caused by multipath delays which approach or exceed the symbol period of the transmitted symbol.

A common rule of thumb to determine if a channel is a frequency selective or not is that the symbol period should be at least ten times smaller than the root mean square delay spread as in (2.14):

$$T_s < 10\ \sigma_\tau \tag{2.14}$$

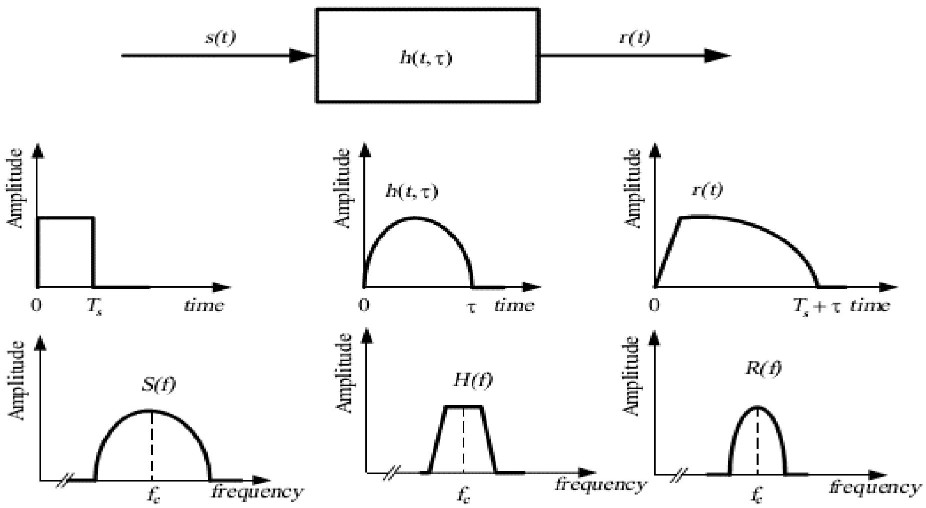

Figure 2.6: Pulse and frequency response shaping by a frequency selective fading channel [25].

2.4.3 Slow Fading

Slow fading sometimes called shadowing is generally caused by buildings, mountains, hills and foliage. The impulse response of channel changes at a rate slower than the transmitted base band signal [27]. In time domain, a channel is generally referred to as introducing slow fading if

$$T_s << T_c \tag{2.15}$$

2.5 Rayleigh Fading

Rayleigh fading occurs due to multipath reception. Usually a large number of reflected and/or scattered waves that arrive at the mobile receiver antenna may add up destructively and the instantaneous received power seen by a moving antenna becomes a random variable. In Rayleigh fading, it is supposed that the magnitude of the signal passing through a transmission medium varies randomly according to the Rayleigh distribution [28]. Figure 2.7 shows the Rayleigh distribution for different various σ^2.

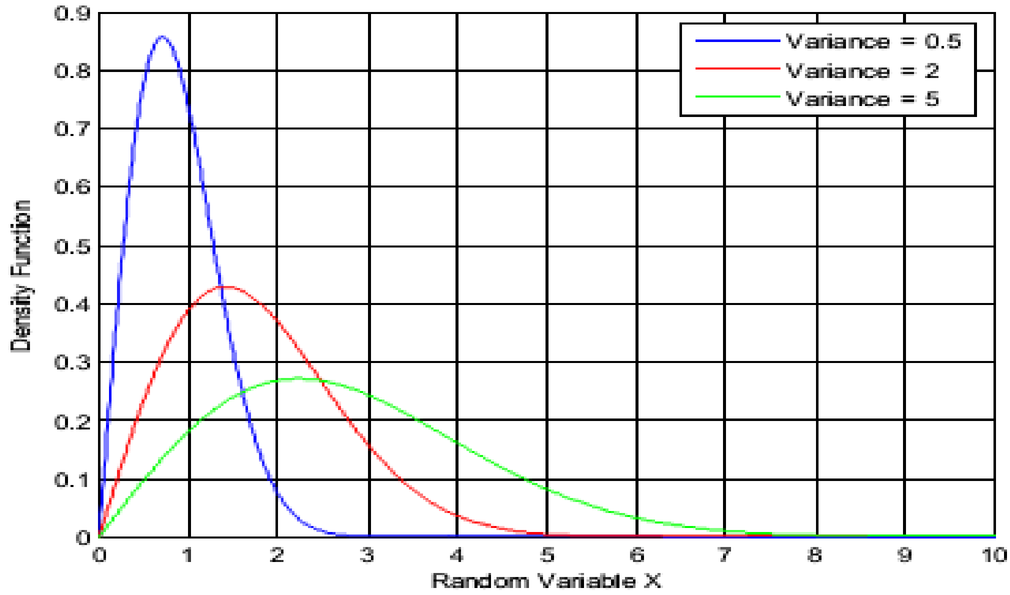

Figure 2.7: Rayleigh Distribution for Different Various [25].

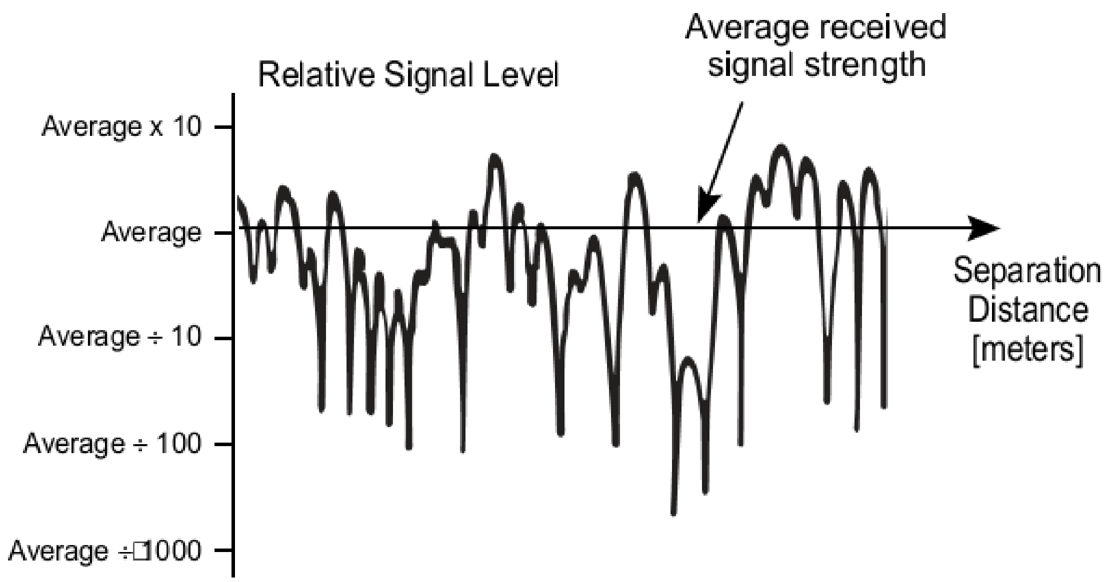

Figure 2.8: Rayleigh Fading Effect [25].

The MS in a radio channel, receives a number of reflected and scattered waves, as well as receive the signal over one line-of-sight path (refer to Fig 2.1). Due to varying path lengths, the amplitude and the phases are random, the instantaneous received power becomes a random variable. Figure 2.8 shows the Rayleigh fading effect on the received signal. If we assume that there is no direct path or line-of sight (LOS) component, the received signal $R(t)$ can be expressed as:

$$R(t) = \sum_{i=1}^{k} \alpha_i \cos(w_c t + \varphi_i) \tag{2.16}$$

Where k represents the number of paths, w_c the frequency of the transmitted signal, α_i is the amplitude for the ith path and $\varphi_i$denotes the phase change of the ith path by 2π when the path length changes by a wavelength. We note that the phases are uniformly distributed over [0,2π].

Rayleigh fading is known to cause deep fades based on the speed of the MS the amount of Doppler shift. Figures 2.9 and 2.10 depict the variations in the received signal power over 1 second after the signal passes through a single-path Rayleigh fading channel with Doppler shifts of 10 Hz and 100 Hz each.

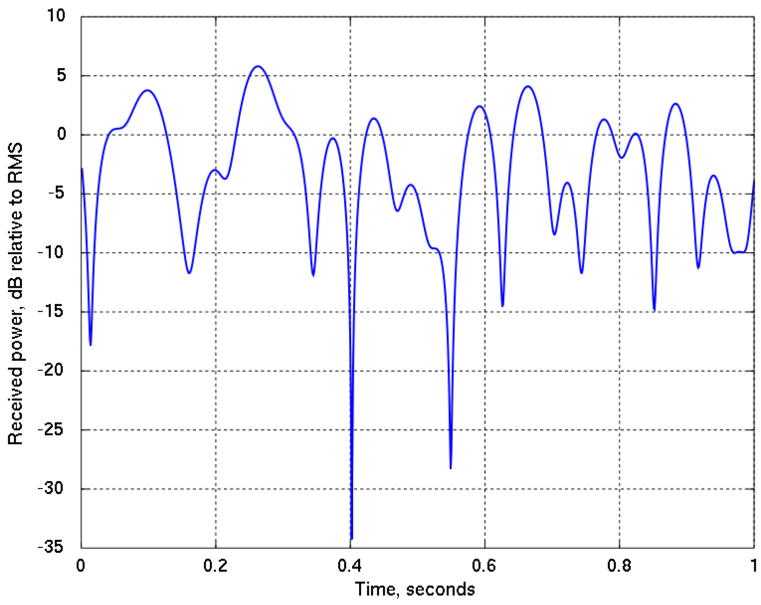

Figure 2.9: Power Variation When Doppler Shift is 10 Hz [25].

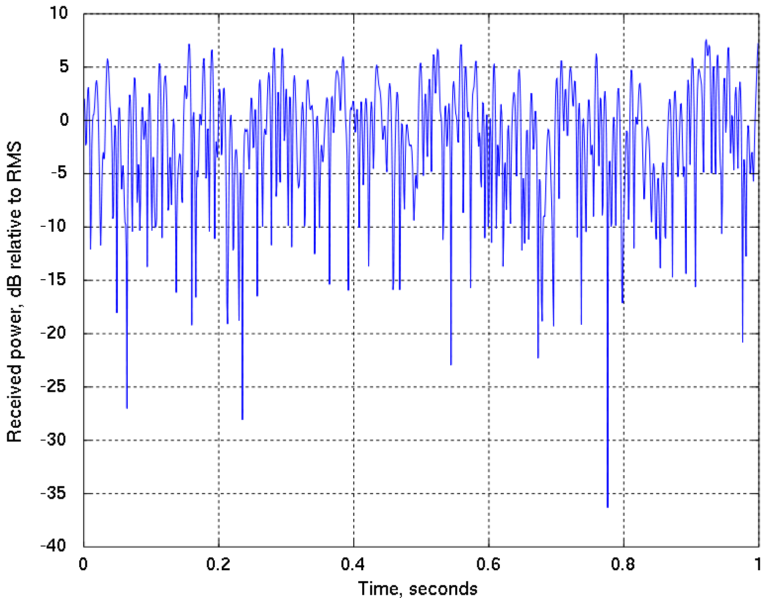

Figure 2.10: Power Variation When Doppler Shift is 100 Hz [25].

Chapter 3

ORTHOGONAL FREQUENCY DIVISION MULTIPLEXING

3.1 Introduction

OFDM is a multi-carrier modulation (MCM) technique. The MCM scheme as the name implies is a modulation technique in which multiple carriers are used for modulating the information signals. It is a suitable modulation used for high data rate transmission and is able to mitigate the effects of inter symbol interference (ISI) and inter carrier interference (ICI). In an OFDM scheme, a huge number of orthogonal, overlapping, narrow band sub-channels, transmitted in parallel sub-dividing the existing transmission bandwidth. The overlapping of the sub-channels do not create any problems since the peak of one subcarrier occurs at zeros of other subcarriers. Orthogonality between the different subcarriers is achieved by using IFFT. Figure 3.1 depicts the spectrum for 5 different frequencies where, $1/_{NT_s}$ is the subcarrier spacing. We clearly see that for the red and green peaks the dashed lines cross from the zero crossings of the other carriers [29].

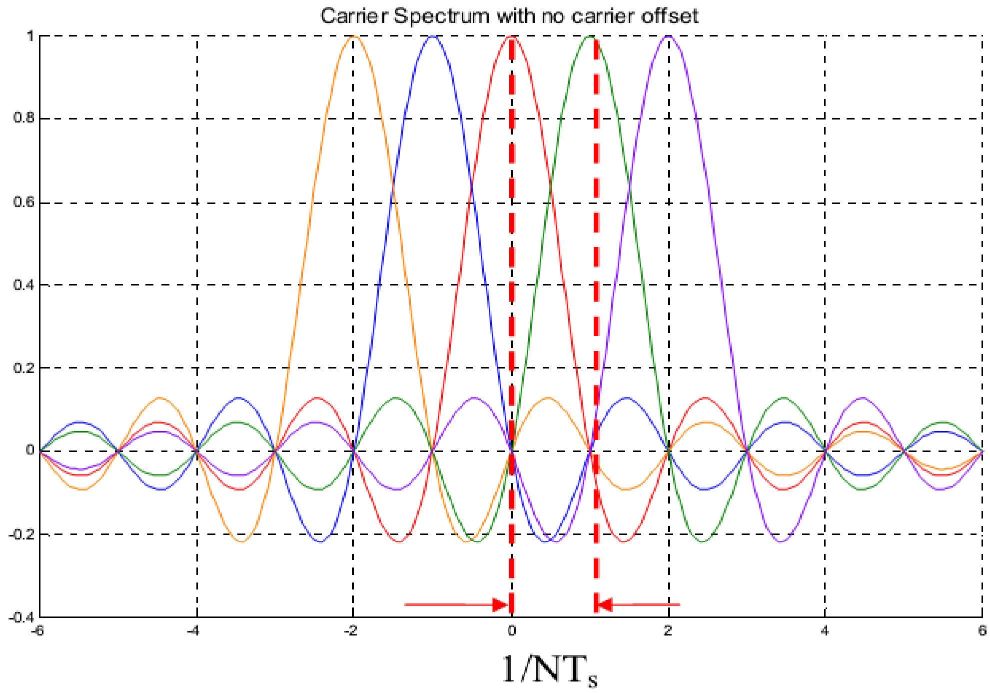

Figure 3.1 : Frequency Spectrum for 5 Orthogonal Subcarriers [29].

3.2 Transceiver of an OFDM System

The general block diagram of an OFDM transceiver has been shown in Figure 3.2. The digital data if first up-converted by a modulation scheme and then the symbols are put into parallel streams that the IFFT block is going to work on [30]. After IFFT is taken an appropriately sized cyclic prefix is appended at the end of the signal. Finally, the signal is sent into the channel. This channel is either the AWGN or the flat fading Rayleigh channel. At the receiver the first task is to remove the cyclic prefix and then apply FFT [30]. Afterwards, the parallel streams are serialized and then the symbols put through the demodulator for obtaining the input source data.

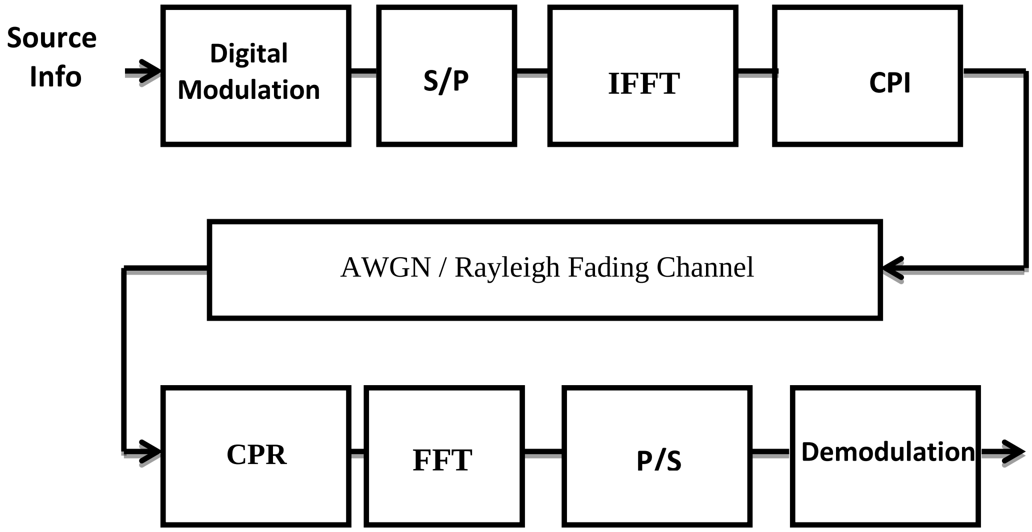

Figure 3.2: OFDM Transmitter- Receiver Block Diagram

Once the cyclic prefix is removed taking IFFT of the signal is equivalent to multiplying the constellation points by sinusoids whose frequencies are equal to the frequency of a carrier signal and then summing these products as depicted by Figure 3.3.

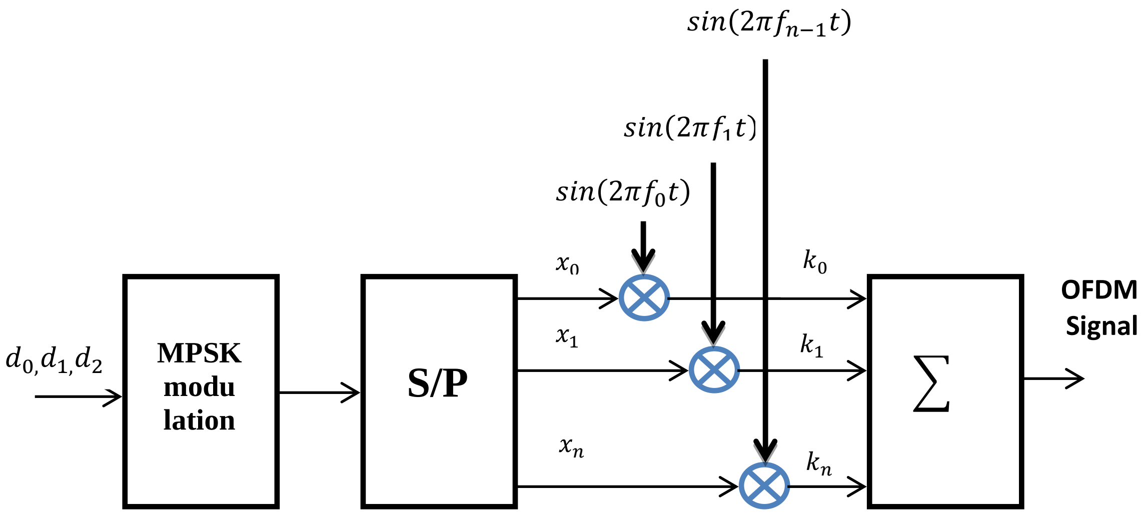

Figure 3.3 : IFFT Processing at the OFDM Transmitter

The frequencies of the different sinusoids are k* (1/T) where $k = 1, \ldots$ n and T is the period of the symbol.

If the symbol rate for the main data stream is R then the data rate on each subcarrier is reduced by a factor of n and becomes

$$R_n = R/n \tag{3.1}$$

And the symbol period T_n on each data bank is

$$T_n = \frac{1}{R_n} = \frac{n}{R} = L \cdot T \tag{3.2}$$

3.2.1 Cyclic Prefix

Most of the time the interference caused by the dispersive channel is reduced by the use of a guard time introduced through the use of a cyclic prefix. For avoiding inter carrier interference in an OFDM system orthogonality between subcarriers must be preserved. This is only possible if time and frequency synchronization is done properly. A delayed production of one subcarrier can interfere with another subcarrier in the next symbol period. This can be avoided by extending the symbol into the guard period that precedes it. The duration of the guard interval must be selected larger than the maximum excess delay time of the radio channel. In such a case, the effective part of the received signal can be seen as the cyclic convolution of the transmitted OFDM symbol with that of the channel impulse response. There are two important benefits of using a cyclic prefix. Firstly, it acts as a guard space between sequential OFDM symbols and help reduce the effect of inter-symbol interference in a fading environment and secondly, it ensures orthogonality between the sub-carriers by keeping the OFDM symbol periodic over the extended symbol duration and hence is good for avoiding inter-carrier interference.

One disadvantage of the Cyclic Prefix is that as stated in [31], based on the duration of the cyclic prefix there would be some loss on SNR. This loss in SNR can be calculated using equation (3.3):

$$SNR_{loss} = -10\log_{10}\left(1 - \frac{T_{cp}}{T}\right), \tag{3.3}$$

Where, T_{cp} is the length of the cyclic prefix and $T = T_{cp} + T_s$ is the length of the transmitted symbol. To minimize the loss of SNR, the CP should not be made longer than necessary. As stated in [32], the width of the guard interval is usually taken as $\frac{1}{4}, \frac{1}{8}, \frac{1}{16}$ $or\, \frac{1}{32}$ times that of the original block length. Figure 3.4 depicts the copying of the tail part of the OFDM symbol to the front of the block.

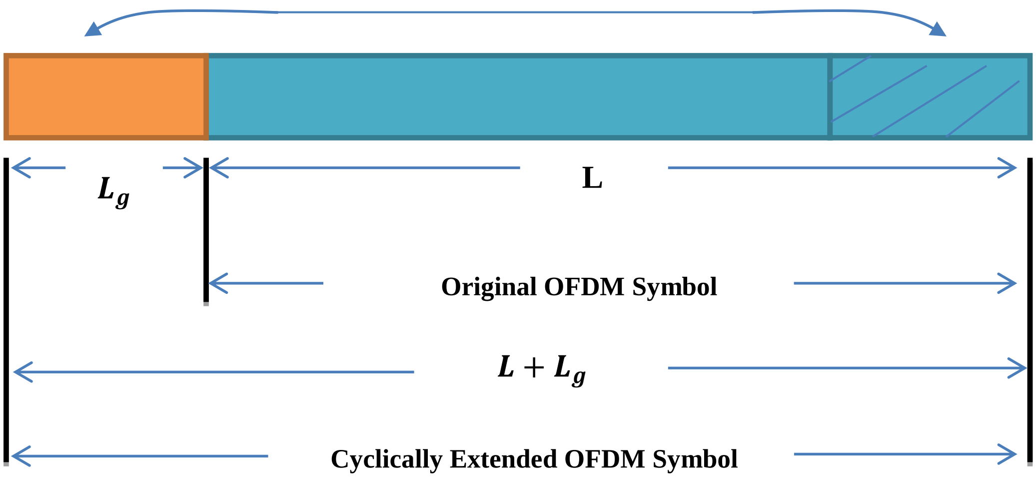

Figure 3.4: Addition of Guard Time by Cyclic Extension.

It is clear that inclusion of a guard interval by cyclic extension would reduce transmission efficiency, however if the useful information blocks are long, the length of the CP will in comparison be low. The efficiency in terms of bit rate capacity can be expressed as given in (3.4):

$$\eta_g = \frac{L}{L + L_g} \tag{3.4}$$

Chapter 4

SPACE-TIME BLOCK CODING

4.1 Introduction

Multiple-input multiple-output (MIMO) system is known to exploit the antenna diversity to develop the performances of wireless communication systems using multiple antenna elements at the transmitter and receiver ends. The main objective of MIMO technology is to improve bit error rate (BER) or the data rate of the communication by applying signal processing techniques at each side of the system. The capacity increases linearly with the number of antennas while using MIMO however it gradually saturates. MIMO can obtain both multiplexing gain and diversity gain and can help significantly increase the system capacity. The earliest studies considering MIMO channels were carried out by Foschini [32] and Telatar [33]. MIMO can be divided into two main classes, spatial multiplexing (SM) and STC.

In a wireless communication system the mobile transceiver has a limited power and also the device is so small in size that placing multiple antennas on it would lead to correlatıon at the antennas due to small separation between them. To avoid this, the better thing to do is to use multiple transmit antennas on the base station and the mobile will have only one. This scenario is known as Multiple Input Single Output (MISO) transmit-diversity. A system with two transmit and one receive antenna is a special case and is known as Alamouti STBC. The Alamouti scheme is well known since it provides full transmit diversity. For coherent detection it is assumed that perfect channel state information is available at the receiver. However, when there is high mobility and the channel conditions are fluctuating rapidly it may be difficult to obtain perfect or close to perfect estimates for the channel. To alleviate this problem another space-time block coding techniques known as DSTBC has been proposed in [34]. In this technique, two serial transmitted symbols are encoded into phase differences and the receiver recovers the transmitted information by comparing the phase of the current symbol with the previously received symbol.

4.2 Transmit Diversity

Transmit diversity (TD) is an important technique to achieve high data rate communications in wireless fading environments and has become widely applied only in the early 2000s. Transmit diversity techniques can be categorized into open loop and close loop techniques [35]. For open-loop systems the most popular transmit-diversity scheme (depicted in Figure 4.2) is the (2x1) Alamouti scheme where channel state information and the code used is known to the receiver.

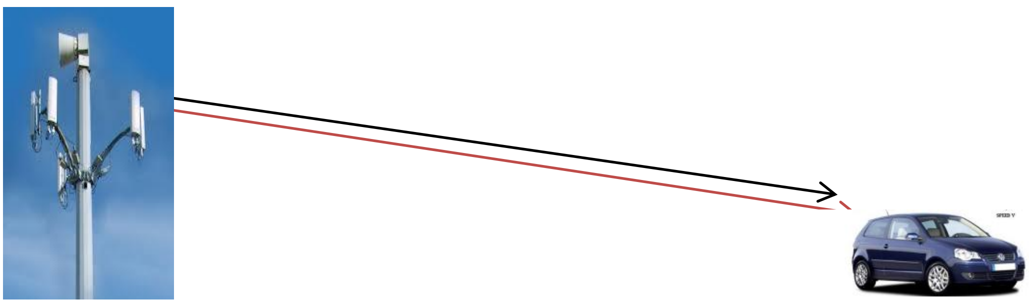

Figure 4.1: Open Loop Transmit Diversity

4.3 Alamouti Code

Alamouti system is one of the first space time coding schemes developed for the MIMO systems which take advantage out of the added diversity of the space direction. Therefore we do not need extra bandwidth or much time. We can use this diversity to get a better bit error rate. At the transmitter side, a block of two symbols is taken from the source data and sent to the modulator. Afterwards, the Alamouti space-time encoder takes the two modulated symbols, in this case x_1 and x_2 and creates an encoding matrix $\boldsymbol{X}$ where the symbol x_1 and x_2 are planned to be transmitted over two transmit antennas in two consecutive transmit time slots.

The Alamouti encoding matrix is as follows:

$$\boldsymbol{X} = \begin{bmatrix} x_1 & x_2 \\ -x_2^* & x_1^* \end{bmatrix} \tag{4.1}$$

A block diagram of the Alamouti ST encoder is shown in Figure 4.2.

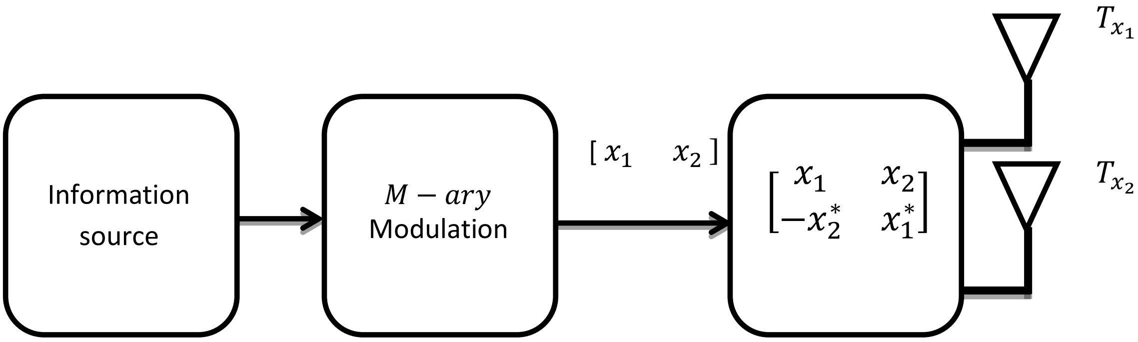

Figure 4.2: Alamouti Space-Time Encoder.

The Alamouti STBC scheme which has 2 transmit and N_r receive antennas can deliver a diversity order of 2 N_r [36]. Also, since for space time codes the rate is defined as R=k/p (where k is the number of modulated symbols the encoder takes as input and p is the number of transmit antennas) for the Alamouti STBC the rate equals 1.

4.4 Alamouti STBC Decoding

4.4.1 Alamouti STBC Decoding with One Receive Antenna

A block diagram of Alamouti STBC decoder is illustrated in Fig. 4.3. At the receiver antenna, the signals r_1 and r_2 received over two consecutive symbol periods can be written as follows:

$$
\begin{aligned}
r_1 &= r(t) = h_1 x_1 + h_2 x_2 + n_1 \\
r_2 &= r(t+T) = -h_1 x_2^* + h_2 x_1^* + n_2
\end{aligned}
\tag{4.2}
$$

In order to estimate the transmitted symbols (two in this case) the decoder needs to obtain the channel state information (in this work we assume we have perfect CSI) and also use a signal combiner as could be seen from Fig 4.3.

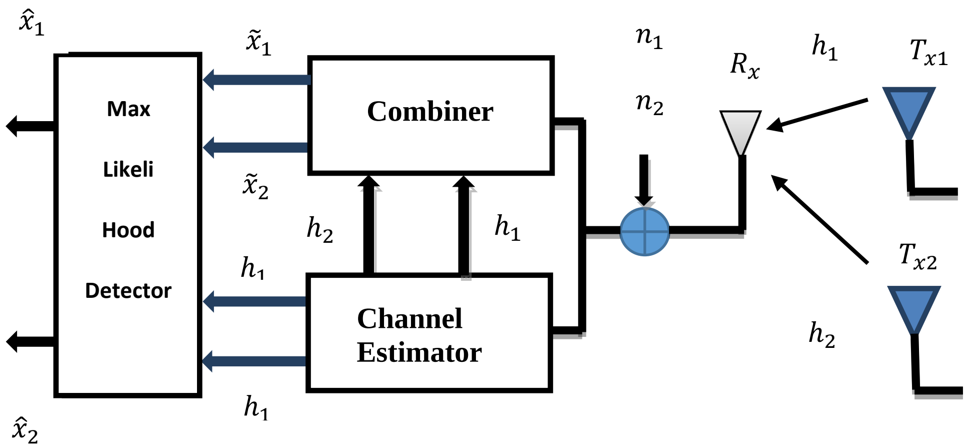

Figure 4.3: Alamouti STBC Decoder

The channel estimates together with the outputs from the combiner are then passed on to the Maximum Likelihood decoder (ML) to obtain the estimates of the transmitted symbols. Considering that all the constellation points are equiprobable, the decoder will choose among all pairs of signals $(\hat{x}_1, \hat{x}_2)$ one that would minimize the distance metric shown below:

$$d^2(r_1, h_1\hat{x}_1 + h_2\hat{x}_2) + d^2(r_2, -h_1\hat{x}_2^* + h_2\hat{x}_1^*)$$

$$= |r_1 - h_1\hat{x}_1 - h_2\hat{x}_2|^2 + |r_2 + h_1\hat{x}_2{}^* - h_2\hat{x}_1{}^*|^2 \quad (4.3)$$

By Substituting (4.2) into (4.3), the maximum likelihood decoding can be written as

$$(\hat{x}_1, \hat{x}_2) = arg \underset{(\hat{x}_1, \hat{x}_2 \epsilon C)}{min} (|h_1|^2 + |h_2|^2 - 1)\,(|\hat{x}_1|^2 + |\hat{x}_2|^2) + d^2(\tilde{x}_1, \hat{x}_1) +$$

$$d^2(\tilde{x}_2, \hat{x}_2) \quad (4.4)$$

Where, C is all probable modulated symbol pairs $(\hat{x}_1, \hat{x}_2)$, $\tilde{x}_1$ and $\tilde{x}_2$ are formed by combining the received signals $r_1 and\ r_2$ with channel state information known at the receiver. The combined signals are given by:

$$\tilde{x}_1 = h_1^* r_1 + h_2 r_2^* \quad (4.5)$$

$$\tilde{x}_2 = h_2^* r_1 - h_1 r_2^*$$

Substituting r_1 and r_2 from (4.2), into (4.5), the combined signals can be written as,

$$\begin{aligned} \tilde{x}_1 &= (|h_1|^2 + |h_2|^2)x_1 + h_1^* n_1 + h_2 n_2^* \\ \tilde{x}_2 &= (|h_1|^2 + |h_2|^2)x_2 + h_1^* n_2 + h_2 n_1^* \end{aligned} \quad (4.6)$$

h_1 and h_2 are a channel realization, the combined signals $\tilde{x}_i$, i =1,2, depends only on x_i, i =1,2. It is possible to split the maximum likelihood decoding rule into two independent decoding rules for $x_1$and x_2 as shown below:

$$\begin{aligned} \hat{x}_1 &= arg \underset{(\hat{x}_1 \epsilon\ S)}{min} (|h_1|^2 + |h_2|^2 - 1)\,|\hat{x}_1|^2 + d^2(\tilde{x}_1, \hat{x}_1) \\ \hat{x}_2 &= arg \underset{(\hat{x}_2 \epsilon\ S)}{min} (|h_1|^2 + |h_2|^2 - 1)\,|\hat{x}_1|^2 + d^2(\tilde{x}_2, \hat{x}_2) \end{aligned} \quad (4.7)$$

Since for M-PSK modulated symbols $(|h_1|^2 + |h_2|^2 - 1)\ |\hat{x}_i|^2$, i = 1, 2 is constant for all signal points equation (4.7) can further be simplified as:

$$\hat{x}_1 = arg \underset{(\hat{x}_1 \epsilon\ S)}{min} d^2(\tilde{x}_1, \hat{x}_1)$$
$$\hat{x}_2 = arg \underset{(\hat{x}_2 \epsilon\ S)}{min} d^2(\tilde{x}_2, \hat{x}_2) \tag{4.8}$$

4.4.2 Alamouti STBC with Two Receive Antennas

Alamouti scheme can also be used for multiple antennas at the receiver to achieve receive diversity. Figure 4.4 shows STBC scheme with two transmit and two receive antennas. Two receive antennas as explained in [6] would increase the diversity gain in comparison to systems with one receive antenna.

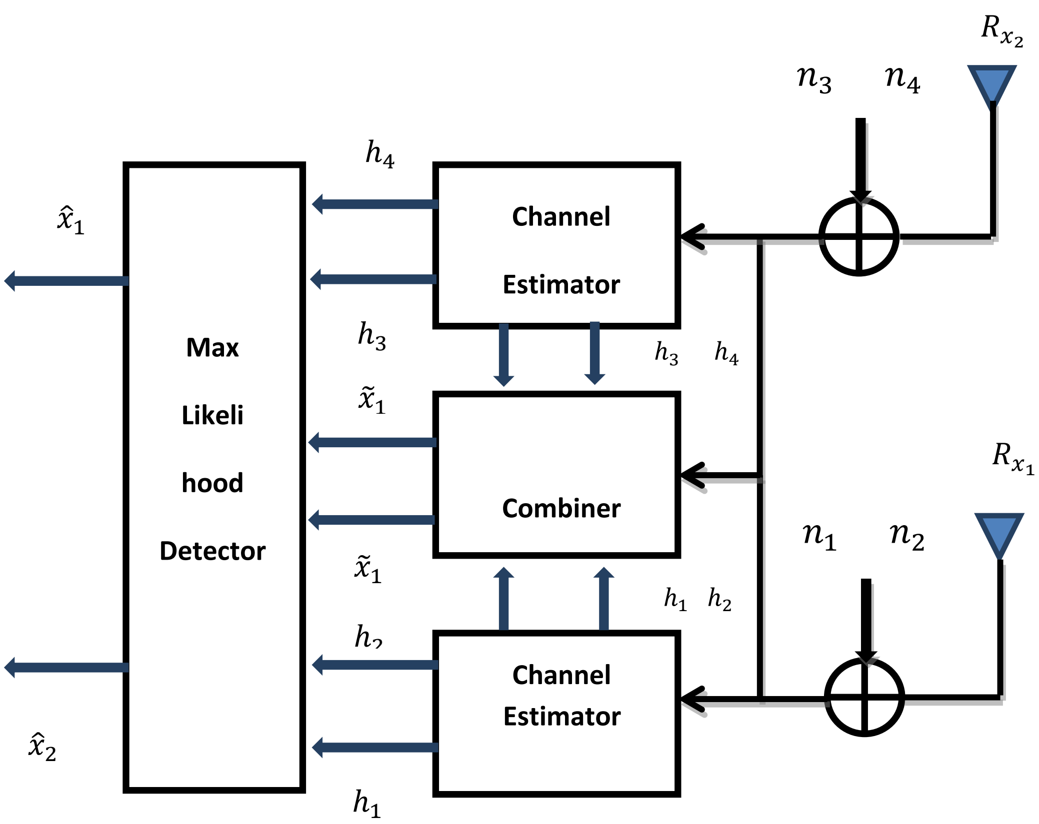

Figure 4.4: Two Branch Transmit Diversity with Two Receive Antennas

The received signals r_1 , r_2, r_3 and r_4 from two receive antennas, can be written as:

$$
\begin{aligned}
r_1 &= h_1x_1 + h_2x_2 + n_1 \\
r_2 &= -h_1x_2^* + h_2x_1^* + n_2 \\
r_3 &= h_3x_1 + h_4x_2 + n_3 \\
r_4 &= -h_3x_2^* + h_4x_1^* + n_4
\end{aligned}
\tag{4.9}
$$

Two combined signals that are sent to the maximum likelihood detector, the combiner in Figure 4.4 generates the following outputs

$$
\begin{aligned}
\tilde{x}_1 &= h_1^*r_1 + h_2r_2^* + h_3^*r_3 + h_4r_4^* \\
\tilde{x}_2 &= h_2^*r_1 - h_1r_2^* + h_4^*r_3 - h_3r_4^*
\end{aligned}
\tag{4.10}
$$

As before the maximum likelihood decoding rule can be written as

$$
\begin{aligned}
\hat{x}_1 &= arg \min_{(\hat{x}_1, \hat{x}_2 \epsilon\, S)} (|h_1|^2 + |h_2|^2 + |h_3|^2 + |h_4|^2 - 1)\, |\hat{x}_1|^2 + d^2(\tilde{x}_1, \hat{x}_1) \\
\hat{x}_2 &= arg \min_{(\hat{x}_1, \hat{x}_2 \epsilon\, S)} (|h_1|^2 + |h_2|^2 + |h_3|^2 + |h_4|^2 - 1)\, |\hat{x}_1|^2 + d^2(\tilde{x}_2, \hat{x}_2)
\end{aligned}
\tag{4.11}
$$

4.5 Differential Space Time Block Coding (DSTBC)

In Differential STBC one can retrieve the transmitted sequence without the need to know the channel estimates. In DSTBC since two successive transmitted symbols are encoded into phase differences, then it is possible for the receiver to recover the transmitted information by comparing the phase of the current symbol with that of the previously received symbols.

4.6 Differential Phase Shift Keying (DPSK)

Encoder block diagram for the DPSK scheme is depicted in Fig. 4.5. The process of DPSK modulation is as follows. First the transmitter sends a random symbol c_0 at time zero. Then at time t, if the input symbol x_t is 1**,** the symbol c_t is left unchanged with respect to the previous symbol. However, when x_t is 0, c_t is changed [16].

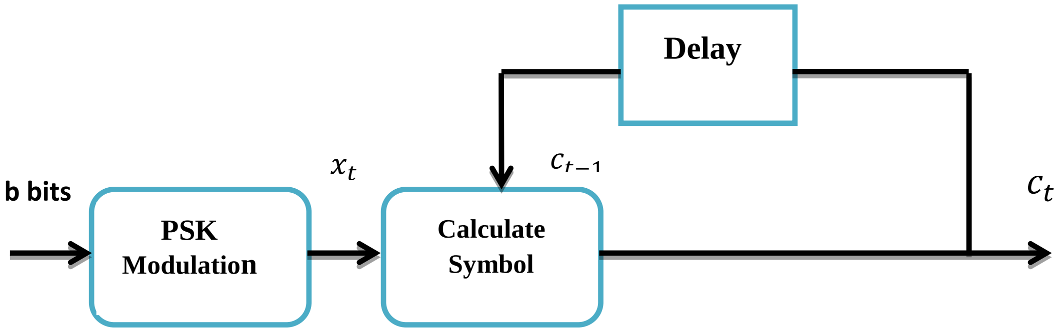

Figure 4.5: DPSK Encoder Block Diagram.

Table 4.1 illustrates the generation of a DPSK signal

Table 4.1: Generation of DPSK Signal

x_t	-	1	0	1	0	0	1	0	1	1	1
c_{t-1}	-	1	1	0	0	1	0	0	1	1	1
c_t	1	1	0	0	1	0	0	1	1	1	1

The decoder in DPSK modulation does not require CSI since the transmitted symbols depend on the previous symbol and the decoder would sense the data from symbols that come one after each other.

The received signal for DPSK can be written as

$$r_t = \delta \cdot c_t + n_t \tag{4.13}$$

where, δ is the gain of the path between the base station and the mobile and n_t is the additive noise in the channel. For the detection of the transmitted symbols at any time t, the receiver would first compute $r_t r_{t-1}^*$ and then compares this value with PSK constellation points to estimates the transmitted symbol (s).

Equation 4.14 shows how the quantity $r_t r_{t-1}^*$ can be computed as explain in [37].

$$r_t r_{t-1}^* = |\delta|^2 c_t c_{t-1}^* + \delta c_t n_{t-1}^* + n_t \delta^* c_t^* + n_t n_{t-1}^*$$

$$\approx |\delta|^2 c_{t-1} x_t c_{t-1}^* \quad + \delta c_t n_{t-1}^* + n_t \delta^* c_{t-1}^* \tag{4.14}$$

$$= |\delta|^2 x_t + N$$

In the above equation N denotes the Gaussian noise, $n_t n_{t-1}^*$ has been ignored since the channel assumed is quasi static. Finally one can obtain an optimal estimate of x_t using eq. (4.15)

$$\hat{x}_t = arg \overset{min}{x_t} | \quad r_t r_{t-1}^* - |\delta|^2 x_t \; |^2 \tag{4.15}$$

In (4.15), $|\delta|^2$ is a constant for PSK symbols since they all have equal power. Hence one can write eq. (4.15) as:

$$\hat{x}_t = arg \overset{min}{x_t} |r_t r_{t-1}^* - x_t|^2 \tag{4.16}$$

4.7 DSTBC Encoder

The motivation to extend differential schemes to MIMO systems, led to the birth of DSTBC schemes. Figure 4.6 shows the block diagram for the DSTBC encoder [37].

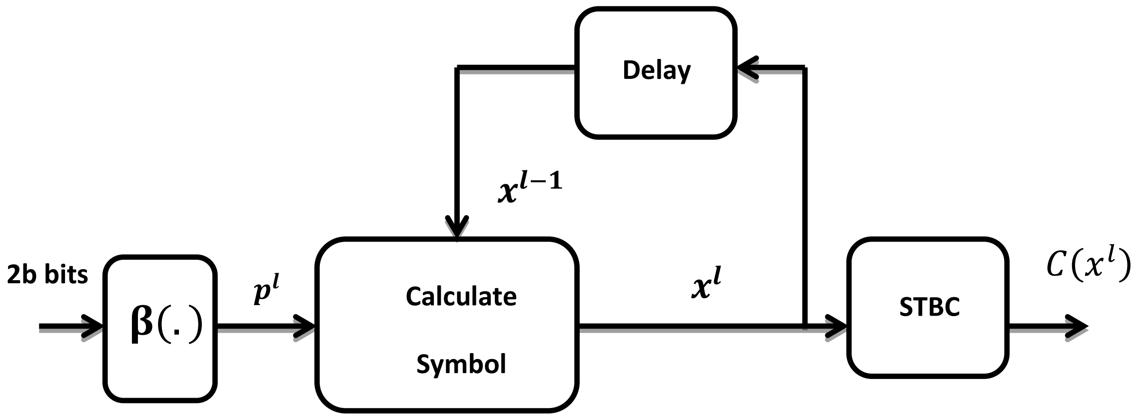

Figure 4.6: DSTBC Encoder Block Diagram

For any given constellation, say A, there are 2^{2m} distinct coefficient vectors that correspond to M^2 distinct signal vectors. If we denote the coefficient vectors by **U**, then as depicted by the figure above each 2b bits of information will be mapped on to **U** by the mapping function $\beta(\cdot)$. It is worth mentioning that the choice of the set **U** and the mapping function $\beta(\cdot)$ is arbitrary. The only requirement is that the magnitude of the vectors P^l must be unity.

For the case of binary phase shift keying the set **U** can be written as:

$$\boldsymbol{U} = \{(1,0)^T, (0,1)^T, (0,-1)^T, (-1,0)^T\} \tag{4.17}$$

The input to the STBC block would then be

$$x^l = \begin{pmatrix} x_1^l \\ x_2^l \end{pmatrix} \tag{4.18}$$

The two vectors that are orthogonal to each other and constitute the coded data to be transmitted from the individual antennas could then be written as

$$U_1(x^l) = \begin{pmatrix} x_1^l \\ x_2^l \end{pmatrix}, \qquad U_2(x^l) = \begin{pmatrix} \left(x_2^l\right)^* \\ -\left(x_1^l\right)^* \end{pmatrix} \tag{4.19}$$

Assuming that x^{l-1} is transmitted for the $(l-1)$ th block, we calculates x^l by

$$x^l = p_1^l U_1(x^{l-1}) + p_2^l U_2(x^{l-1}) \tag{4.20}$$

4.8 DSTBC Decoder

This section provides the block diagram for the DSTBC decoder for the case of two transmit and one receive antenna.

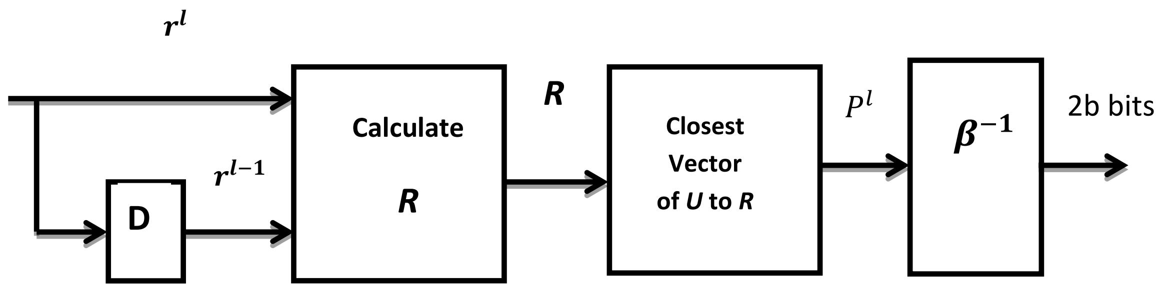

Figure 4.7: Differential Space-Time Decoder

For block l the two received signals would be r_1^l and r_2^l as depicted below

$$r_1^l = \delta_1 x_1^l + \delta_2 x_2^l + n_1^l$$
$$r_2^l = \delta_1 (x_2^l)^* + \delta_2 (x_1^l)^* + n_2^l \tag{4.21}$$

Here, n_1 and n_2 are the noise samples for block l. It is then possible to obtain a noisy version of the vector P^l using the R vector defined below:

$$R = \begin{cases} \hat{x}_1^l = (r_1^{l-1})^* r_1^l + r_2^{l-1} (r_2^l)^* \\ \hat{x}_2^l = (r_2^l)^* r_1^{l-1} - r_1^l (r_2^{l-1})^* \end{cases} = (|\delta_1|^2 + |\delta_2|^2) P^l + N \tag{4.22}$$

The decoder would then find the closest match for the vector P^l in U and consider this matching vector as the estimate of the transmitted vector. Finally to decode the *2b* bits, the estimate vector is reverse mapped using the inverse mapping function $\beta(\cdot)^{-1}$ [38].

Chapter 5

LINK LEVEL PERFORMANCE

In this section we will be presenting the link level performance of STBC and DSTBC coded OFDM using either BPSK or QPSK modulation. All simulations have been carried out using the readily available MATLAB platform and writing dedicated functions for different parts. The simulation results obtained have been presented in four parts. The first part provides the bit error rate performance for BPSK modulated data transmitted over a Rayleigh fading channel. This is then followed by a performance analysis of OFDM over the AWGN channel using either BPSK or QPSK modulation. Third part demonstrates the BER vs. SNR for Alamouti STBC and Alamouti DSTBC coded data transmitted over a Rayleigh fading channel without using OFDM. Finally, part four will provide STBC and DSTBC coded OFDM performance when BPSK and QPSK are the preferred modulation and the channel is again the Rayleigh fading channel.

5.1 Transmission of BPSK Modulated Data Over a Non-Line-of Sight (NLOS) Fading Channel.

When there is a direct path between the transmitter and receiver the channel is usually referred to as the Rician channel and when LOS component is missing it will be referred to as the Rayleigh fading channel. In this section we demonstrate the BER performance of BPSK modulated data over a single path Rayleigh fading channel. Figure 5.1 shows both the simulation and the theoretically obtained results for the AWGN and Rayleigh channels. The analytical expression for the BER for BPSK modulated data in a Rayleigh fading channel is as in (5.1):

$$P_b = 0.5\left(1 - \sqrt{\frac{(E_b/N_0)}{(E_b/N_0)+1}}\right) \tag{5.1}$$

and for the AWGN channel P_b is defined as:

$$P_b = 0.5\, erfc\left(\sqrt{\frac{E_b}{N_0}}\right) \tag{5.2}$$

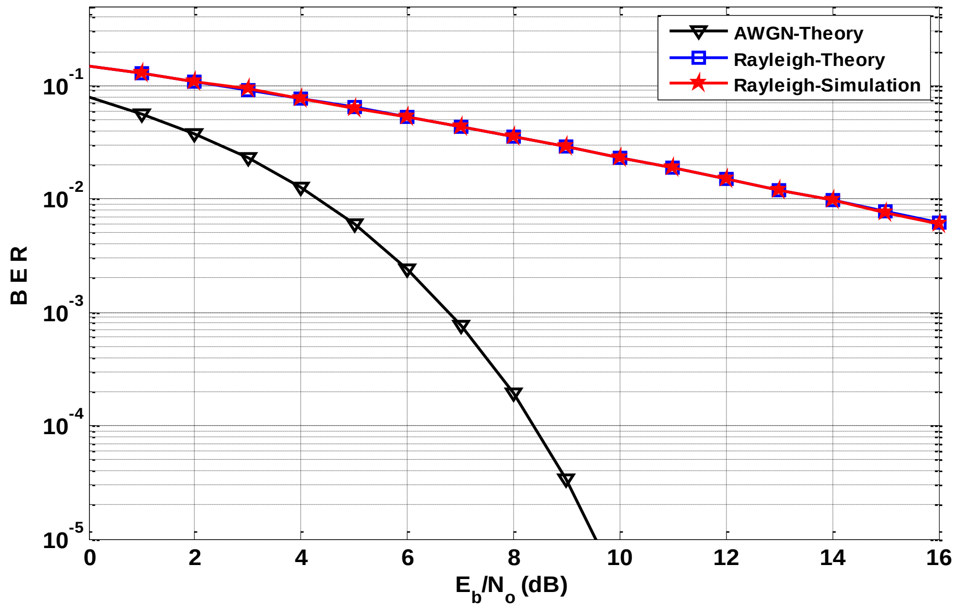

Figure 5.1: BER Plot of BPSK Modulated Data in Rayleigh Fading Channel

From Figure 5.1 we can easily see that, when the channel is a fading channel around 10 dB degradation is experienced due to the multipath effect (in comparison to AWGN, at a BER of 10^{-2}). During simulations 10^6 samples were assumed for the Rayleigh distribution. We note that the simulated and the theoretical results coincide.

5.2 OFDM Using BPSK and QPSK Over the AWGN Channel

OFDM is a medium access technology that is an improved form of spectrally efficient multi-carrier modulation (MCM) technique that employs densely spaced orthogonal subcarriers and overlapping spectrums. Combination of multiple low data rate sub-carriers in OFDM provides a composite high data rate with relatively long symbol duration. Based on the channel coherence time this may help reduce or completely eliminate the interference between symbols due to multipath effect.

This section provides the BER performance for OFDM using both BPSK and QPSK modulation and the simulation parameters given in Table 5.1.

Table 5.1: OFDM System Parameters as defined in IEEE 802.11a [39]

Parameter	**Value**
FFT size	64
Number of used subcarriers.	52
FFT Sampling frequency	20MHz
Subcarrier spacing	312.5kHz
Used subcarrier indexes	{-26 to -1, +1 to +26}
Cyclic prefix duration, T_{cp}	0.8 µs
Data symbol duration, T_d	3.2 µs
Total Symbol duration, T_s	4 µs
Modulation method	BPSK,QPSK

The BER performance of an OFDM system using BPSK and QPSK modulation when the channel is the AWGN channel has been shown in Figures 5.2 and 5.3

respectively. The theoretical results can be produced by using the analytical formulas given in equations (5.3) and (5.4):

$$P_{b,BPSK} = 0.5\, erfc\left(\sqrt{\frac{E_b}{N_0}}\right) \equiv Q\left(\sqrt{\frac{2E_b}{N_0}}\right) \tag{5.3}$$

For BPSK since there is only one bit per symbol, this is also the symbol error rate. Although QPSK can be viewed as a quaternary modulation, the probability of bit-error for QPSK is the same as for BPSK and can be written as:

$$P_b = Q\left(\sqrt{\frac{2E_b}{N_0}}\right) \tag{5.4}$$

In order to achieve the same bit-error probability as BPSK, QPSK uses twice the power (since two bits are transmitted simultaneously). If the signal-to-noise ratio is high, the probability of symbol error may be approximated as:

$$P_s \approx 2Q\left(\sqrt{\frac{E_s}{N_0}}\right) \tag{5.5}$$

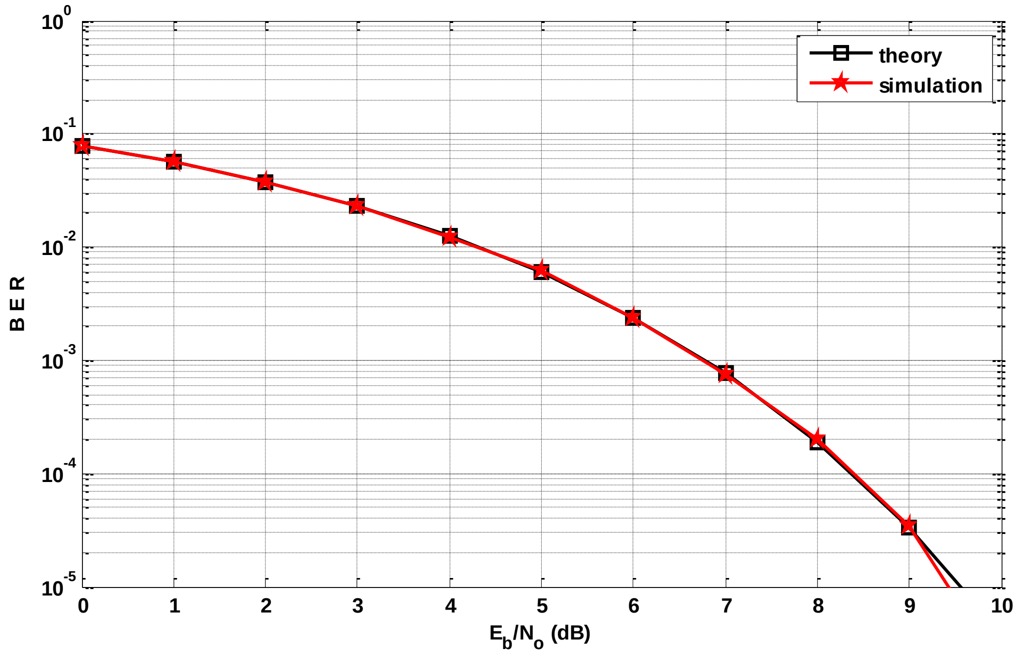

Figure 5.2: BER for OFDM Using BPSK Modulation (AWGN Channel).

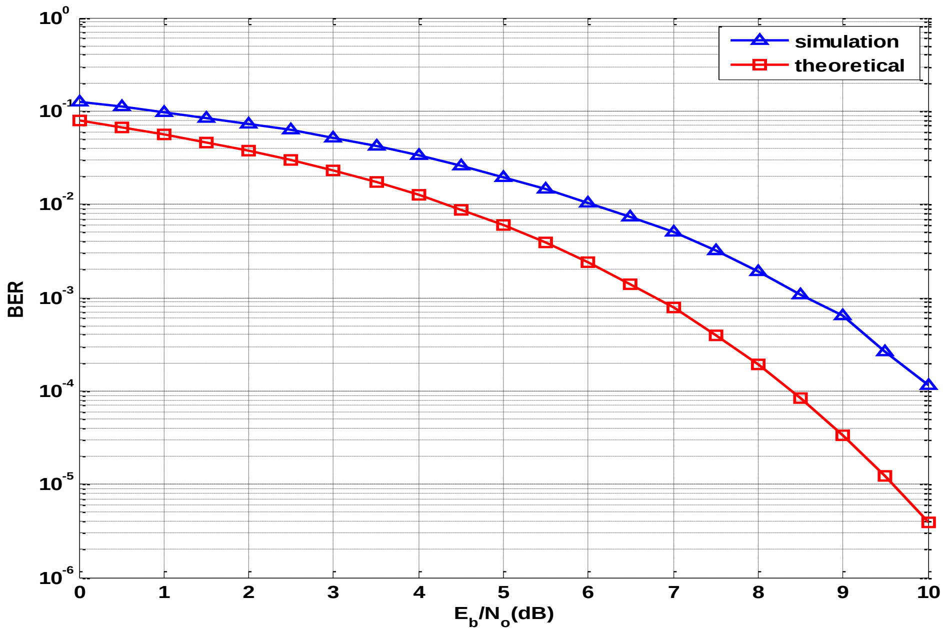

Figure 5.3: BER for OFDM Using QPSK Modulation (AWGN Channel).

5.3 Performance Analysis of Alamouti STBC and DSTBC Coded Data Transmission Over Rayleigh Faded Channels

The advantage in multiple antenna schemes is that they use a new dimension called space in addition to time. Multiplexing gain, antenna gain and diversity gain are three main benefits of MISO and MIMO type systems. Alamouti scheme is known as the first STBC. It uses two transmit antennas and N_r receive antennas. Alamouti STBC has a unity rate and can attain a diversity order of $2 * N_r$. DSTBC is referred to as differential STBC and main difference from the Alamouti STBC is that the encoder would encode the data sequence in a differential manner. DSTBC is generally used when no information is available about the channel. In DSTBC since two successive transmitted symbols are encoded into phase differences, then it is possible for the receiver to recover the transmitted information by comparing the phase of the current symbol with that of the previously received symbols.

This section will provide BER analysis for Alamouti STBC and DSTBC over slow fading Rayleigh channels. For both schemes the simulations have been carried out using two transmit and one receive antenna. The simulation results obtained for STBC and DSTBC have been provided in Figures 5.4, 5.5, 5.6 and 5.7 respectively. Figure 5.4 provides BER vs SNR results for transmit diversities of (2×1) and (2×2) Alamouti STBC. The red curve is the theoretically obtained BER performance for (2 × 1) transmit diversity for STBC when BPSK modulation is assumed. In [40] it has been shown that the probability of error for (2×1) STBC can be obtained using:

$$P_{e,STBC} = p_{STBC}^2[1 + 2(1 - p_{STBC})] \tag{5.6}$$

where,

$$p_{STBC} = \frac{1}{2} - \frac{1}{2}\left(1 + \frac{2}{E_b/N_0}\right)^{-1/2} \tag{5.7}$$

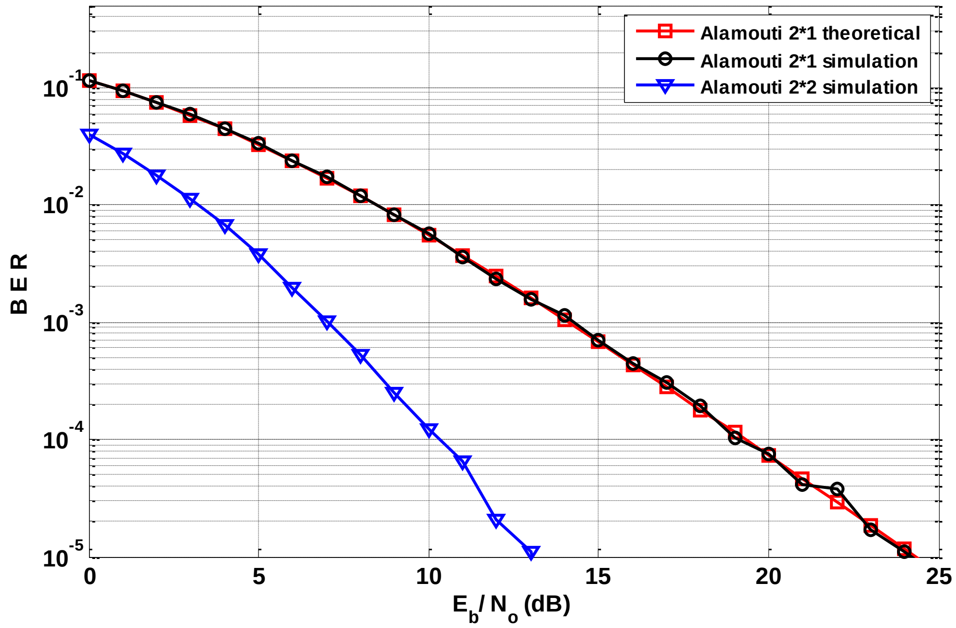

Figure 5.4: BER Over a Rayleigh Fading Channel When 2×1 and 2×2 Alamouti STBC Using BPSK are Employed.

We see that the (2×2) Alamouti STBC would outperform the (2×1) scheme. For a BER value of $10^{-3}$the difference between the (2×1) and (2×2) schemes is around 7dB.

In Figure 5.5 a comparison of (2×1) STBC for BPSK vs. QPSK has been provided. We note that for BER value of 10^{-3} the (2×1) Alamouti STBC using BPSK performs 4.2dB better than (2×1) Alamouti STBC using QPSK. The reason for getting better results with BPSK is that the fading fluctuation often causes two bits error per symbol with QPSK while it causes at most one bit error per symbol with BPSK.

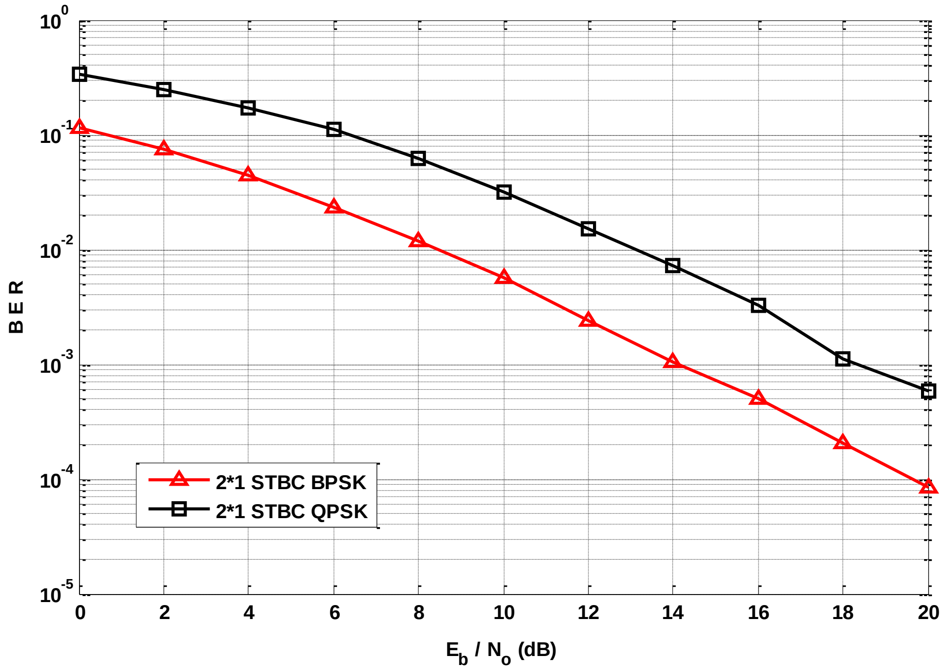

Figure 5.5: (2×1) Alamouti STBC Using BPSK and QPSK

Figure 5.6 depicts the (2×1) STBC versus (2×1) DSTBC BER performance over a slow fading Rayleigh channel using BPSK. We see that the DSTBC in comparison to STBC is always inferior. This difference is mainly because DSTBC has no information about the CSI.

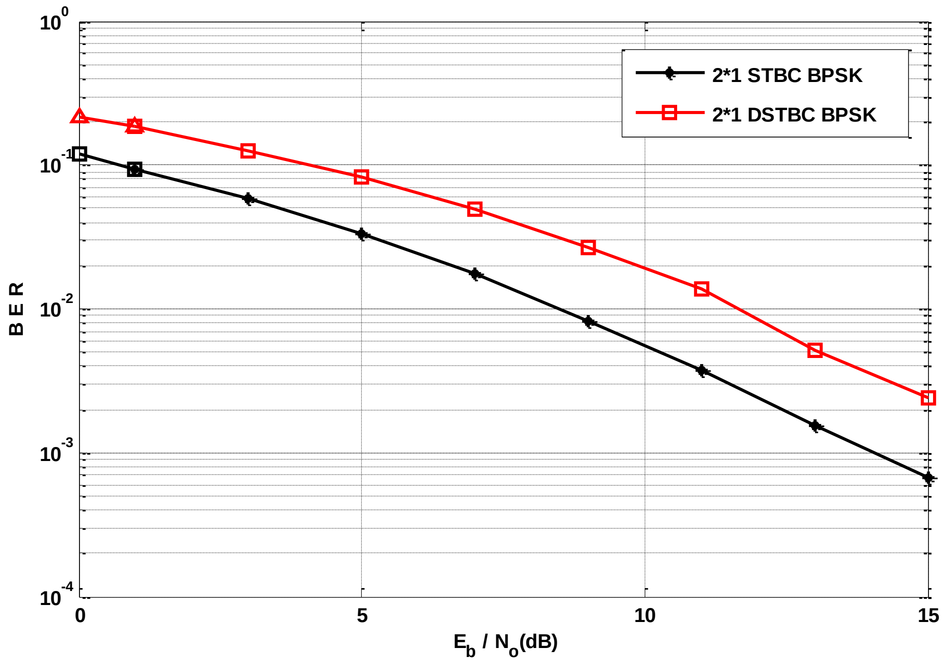

Figure 5.6: BER Comparison between STBC and DSTBC Using BPSK Modulation.

Figure 5.7 depicts the (2×1) STBC versus (2×1) DSTBC BER performance over a slow fading Rayleigh channel while using QPSK. Similar to results depicted in Figure 5.6, the DSTBC performance is always worse than the STBC performance.

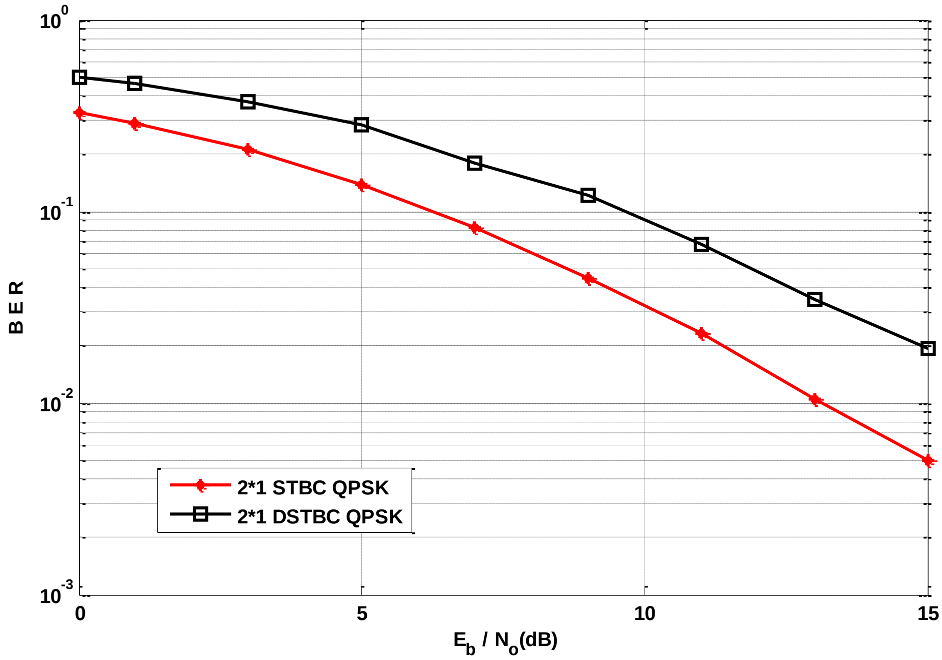

Figure 5.7: BER Comparison between STBC and DSTBC with QPSK.

5.4 Performance of Alamouti STBC-OFDM and Differential STBC-OFDM Over Slow Fading Rayleigh Channels

This section will provide simulation results in three parts. In the first part the BER performance for STBC and DSTBC with and without OFDM will be provided when BPSK or QPSK modulation is used. Part two will then provide a performance comparison between (2×1) STBC-OFDM using BPSK and QPSK. Finally in part three the (2×1) DSTBC-OFDM performance will be compared for BPSK and QPSK modulations. As before the channel will be assumed as slow-fading Rayleigh channel. The OFDM parameters adopted in the simulations are as in Table 5.2.

Table 5.2: OFDM System Parameters for A-STBC OFDM and DSTBC-OFDM

Parameter	**Value**
FFT length	1024
Number of parallel channel	512
Number of carrier	512
Guard Time	28.07 µs
Length of guard interval	128
Modulation	BPSK, QPSK
Transmit Antenna	2
Receive Antenna	1

Figure 5.8 (a), (b) shows the bit error rate performance for STBC vs. STBC together with OFDM when the modulation is either BPSK or QPSK. Similarly Figure 5.9 (a), (b) shows the bit error rate performance for DSTBC vs. DSTBC together with OFDM. In both cases (using either STBC or DSTBC) using OFDM as the medium access technology help improve the results greatly. In fact, for BER value of 10^{-3} using OFDM together with STBC coding would bring an extra gain of ~4.2dB in case of BPSK modulation. We also note that the gain higher for larger SNR values and less at lower SNR values.

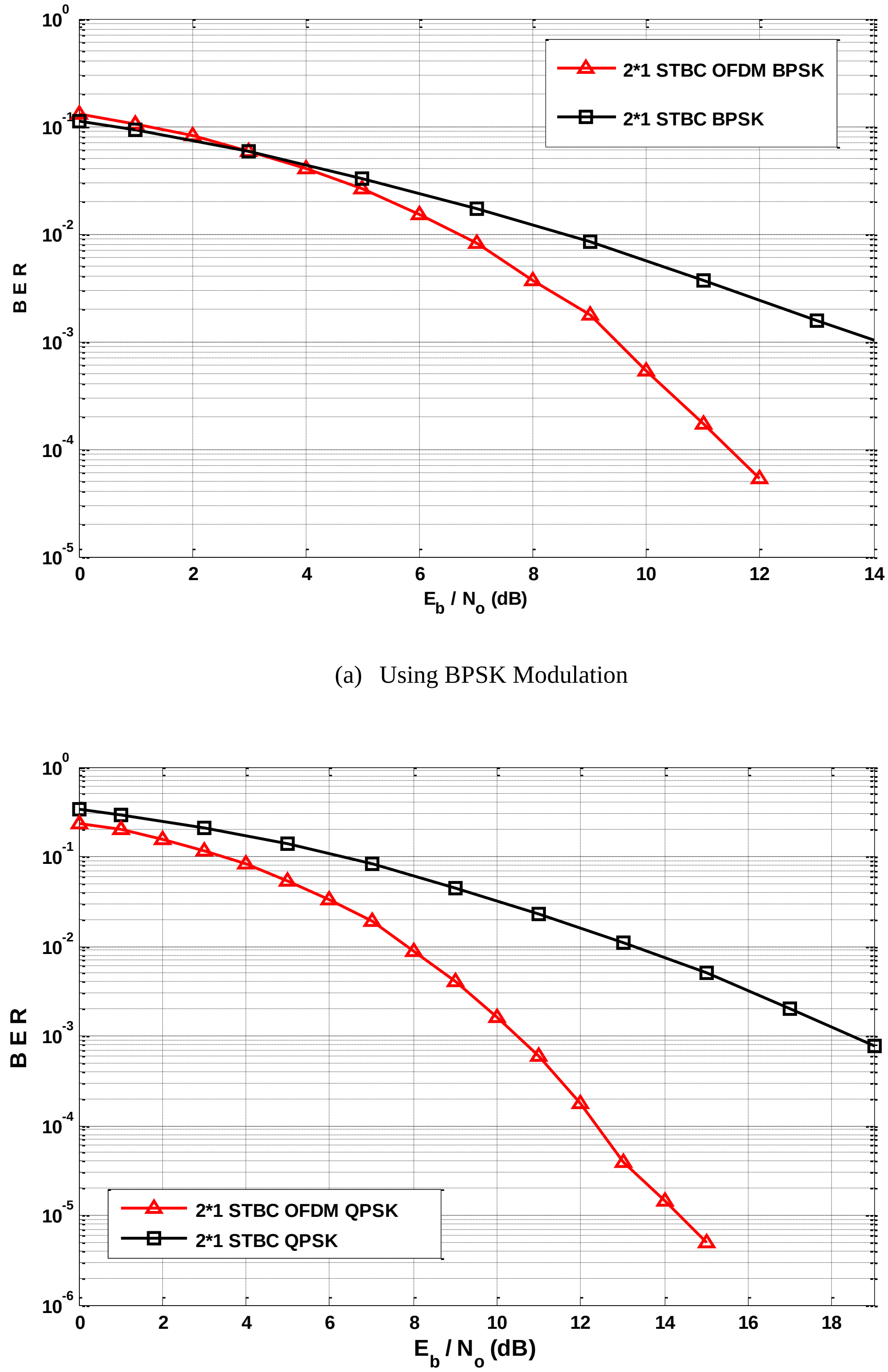

(a) Using BPSK Modulation

(b) Using QPSK Modulation

Figure 5.8: BER Performance of STBC with and without OFDM

Similar performance gain is observed also for DSTBC coupled with OFDM.

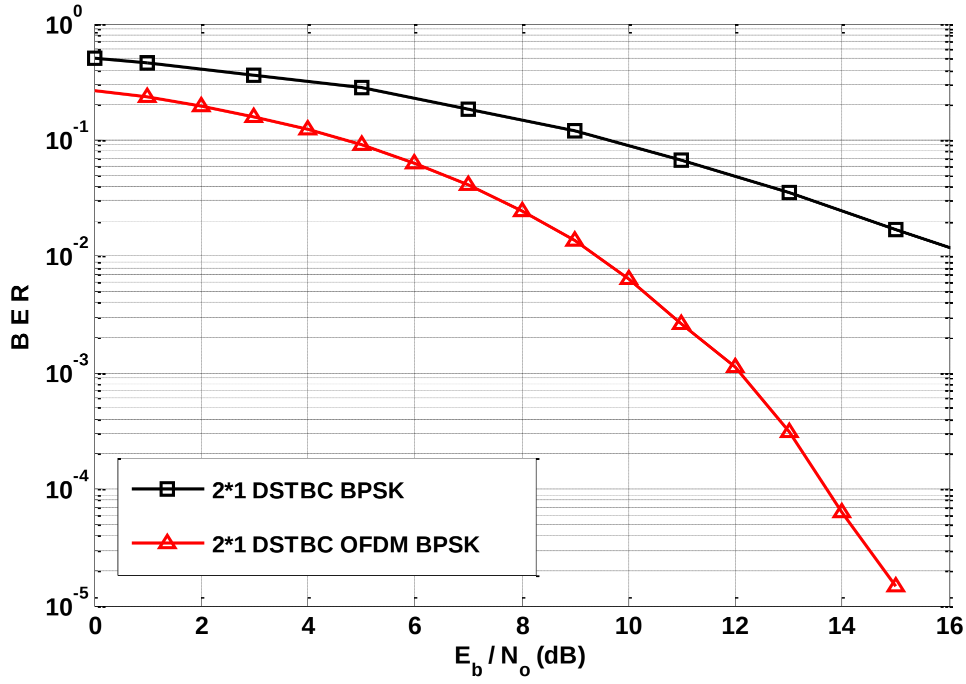

(a) Using BPSK Modulation

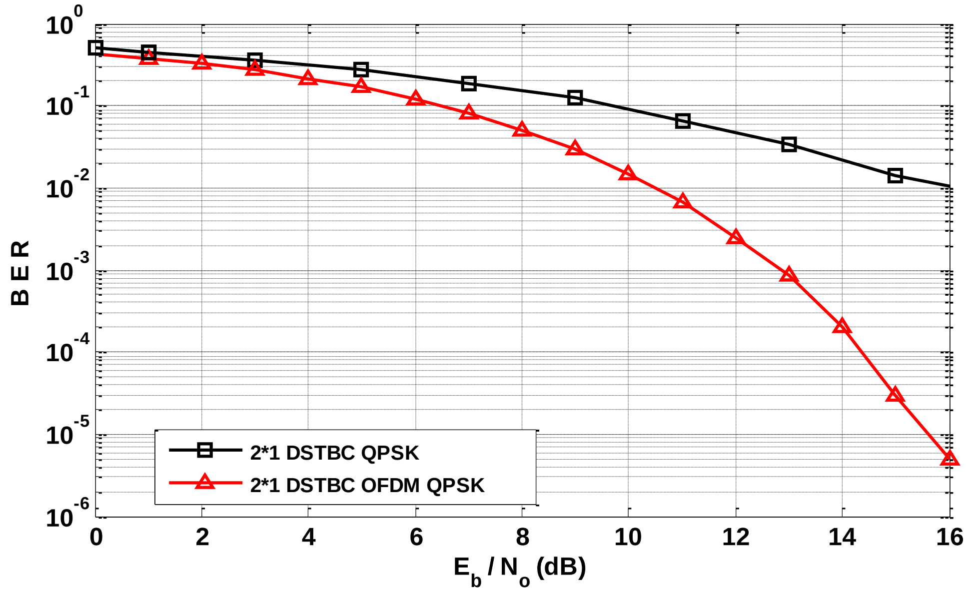

(b) Using QPSK Modulation

Figure 5.9: BER Performance of DSTBC with and without OFDM

Figures 5.10 and 5.11 depict the STBC-OFDM and DSTBC-OFDM BER performances comparatively for BPSK and QPSK. Due to lack of CSI the DSTBC-OFDM results are worse than the STBC-OFDM schemes.

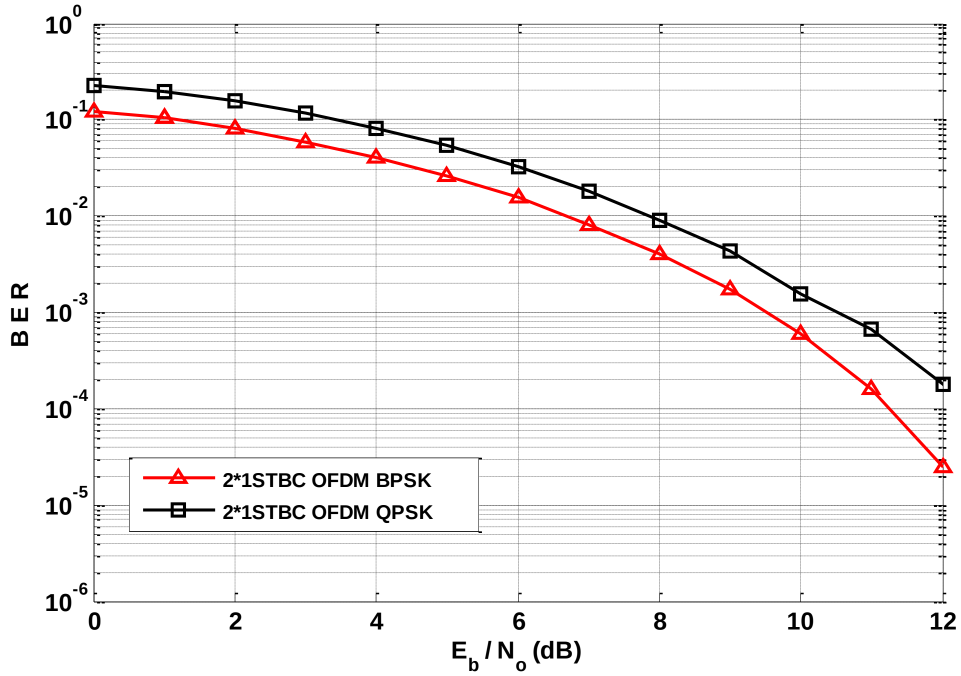

Figure 5.10: BER for Alamouti STBC-OFDM over Slow Fading Rayleigh Channel.

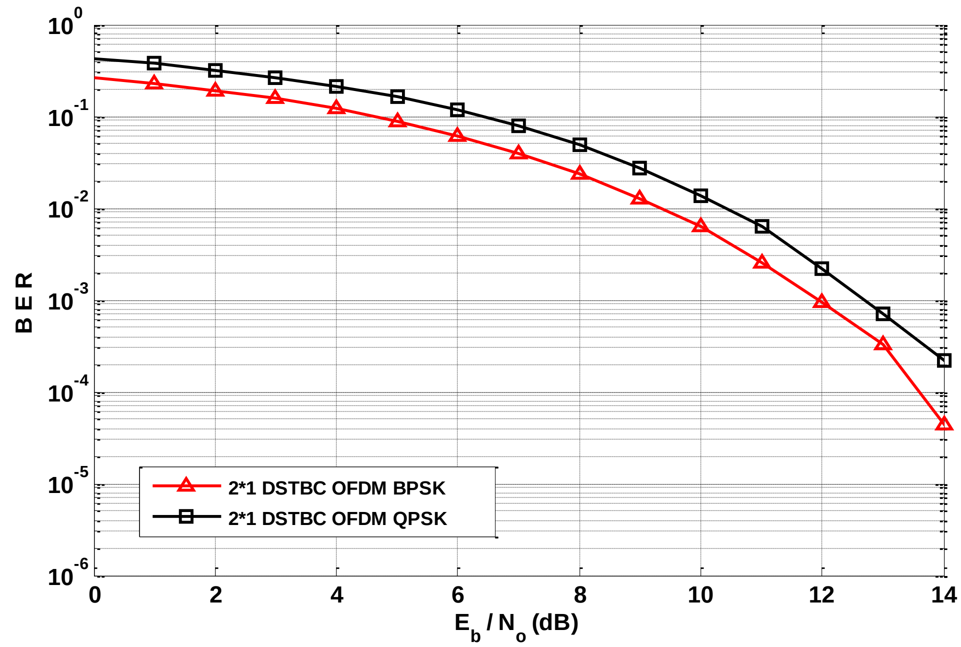

Figure 5.11: DSTBC -OFDM performance over slow fading Rayleigh channel with BPSK and QPSK modulation.

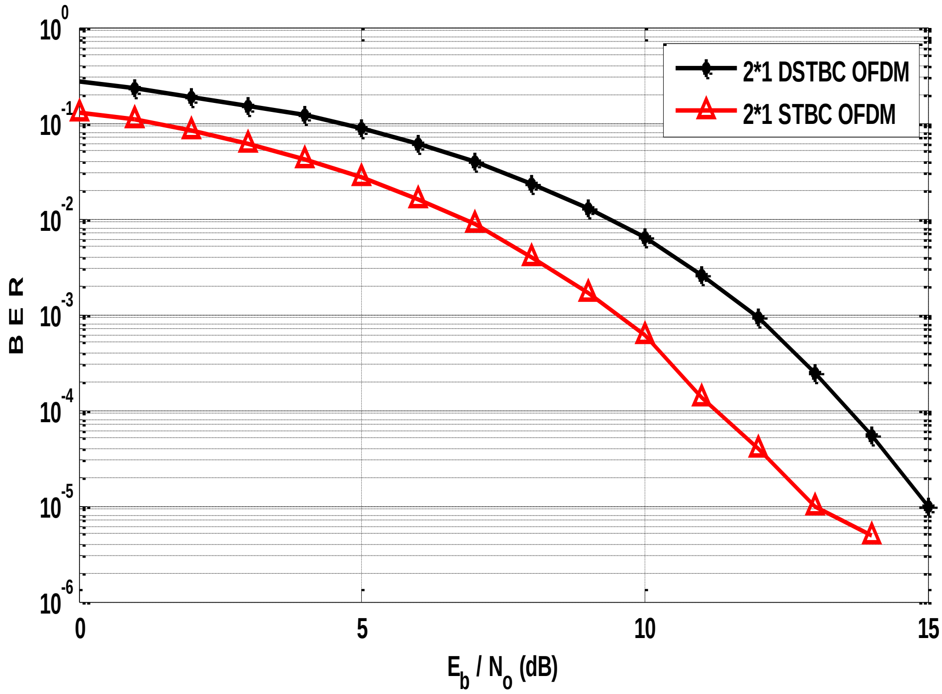

Figure 5.12: STBC-OFDM and DSTBC-OFDM Performance over Slow Fading Rayleigh Channel with BPSK Modulation.

Figure 5.12.depicts the STBC-OFDM and DSTBC-OFDM BER performances comparatively for BPSK. The DSTBC-OFDM results are worse than the STBC-OFDM schemes.

Clearly the usage of a multiple access technology like OFDM helps further to improve the BER results obtained by STBC and DSTBC schemes. The performance increment becomes possible since OFDM combines multiple low data rate streams to create a composite high data rate with relatively long symbol duration. The usage of a guard interval would also help reduce or completely eliminate the interference between symbols due to multipath effect.

Chapter 6

CONCLUSIONS AND FUTURE WORK

6.1 Conclusions

In this thesis we first compared the BER performance of 2×1 and 2×2 transmit diversity STBC data transmission over a Rayleigh fading channel using both BPSK and QPSK modulation. Results with BPSK modulation indicate that using two antennas at the receiver instead of one will bring approximately an extra gain of 9dB at a BER value of 10^{-4}.

Also comparison between 2×1 STBC using BPSK and 2×1 STBC using QPSK indicate that STBC with BPSK modulation would be ~4.2 dB better than the 2×1 STBC with QPSK for BER value of 10^{-3}. These results indicate that to get a better performance over a Rayleigh fading channel MIMO approach would be better than MISO case and low level modulation should be preferred.

In the second phase of the simulations, transmission of data encoded using STBC vs. DSTBC over a Rayleigh fading channel was compared. Since the STBC scheme makes use of a channel estimate and DSTBC does not for both BPSK and QPSK modulations, the BER performance for STBC was better than that of the DSTBC encoded data. This however does not mean that DSTBC should not be considered. In fact when there is high mobility and the channel conditions are fluctuating rapidly it may be difficult to obtain estimates for the channel and the detection of transmitted symbols must be done incoherently. This is possible with an increase in BER performance. For our simulations this degradation was around 3dB both for BPSK and QPSK.

In the third phase of the simulations the transmit diversity schemes were combined with the OFDM scheme and STBC-OFDM vs. DSTBC-OFDM BER performance was obtained over a Rayleigh fading channel. The usage of a multi-carrier modulation technique was seen to further improve the BER results obtained when data was transmitted after encoding by STBC or DSTBC. For both BPSK and QPSK modulations the boost introduced to the BER performance by combining OFDM with the chosen transmit-diversity technique would become more significant after 6dB. At a BER of 10^{-3} this difference in gain is around 4.5dB for STBC OFDM using BPSK and ~6dB for STBC OFDM using QPSK modulation. Then 2×1 DSTBC and OFDM is used back to back similar behavior is experienced however the BER performances are higher due to the fact that detection is done incoherently. The improvement in BER performance when OFDM is used mainly comes due to the use of the guard interval. When the duration of the guard interval is selected larger than the maximum excess delay time of the radio channel this will help reduce the inter-symbol interference in a fading environment and help improve the BER results. Secondly since OFDM splits a broadband channel into multiple sub-channels this changes the behavior of each sub-channel to be flat fading and hence better performance can be observed.

6.2 Future Work

The work described herein mainly concentrated on MIMO-OFDM based systems. However the 4th Generation (4G) communication systems must adopt OFDMA, a multi user version of OFDM as the IMT-Advanced standard dictates. Therefore the future work will involve simulating OFDMA physical layer along with MIMO transmit and receive diversity techniques.

Also some effective channel coding schemes like Convolutional Coding (CC), Turbo Coding (TC) or Low Density Parity Check (LDPC) coding could be employed for providing the flexibility of detecting and correcting errors that may occur during transmission. In information theory, TCs are a class of high-performance forward error correction (FEC) codes developed by Berrou in 1993. Via the use of these TCs performances that approach the channel capacity are possible. TCs have found use in 3G mobile communications and (deep space) satellite communications as well as other applications where designers seek to achieve reliable information transfer over bandwidth- or latency-constrained communication links in the presence of data-corrupting noise. A good competitor of TCs is the LDPC codes, which provide similar performance.

REFERENCES

[1] A. Wittneben, "A new bandwidth efficient transmit antenna modulation diversity scheme for linear digital modulation," *in Proc. IEEE International Conf. Communications (ICC'93)*, pp. 1630–1634, May 1993.

[2] A. Wittneben, "Base station modulation diversity for digital simulcast," *in Proc. IEEE Vehicular Technology Conf. (VTC 41st)*, pp. 848–853, May 1991.

[3] N. Seshadri and J. H. Winters, "Two signaling schemes for improving the error performance of FDD transmission systems using the transmitter antenna diversity," *in Proc. IEEE Vehicular Technology Conf. (VTC43rd)*, pp. 508–511, May 1993.

[4] V. Tarokh, N. Seshadri, and A. R. Calderbank, "Space-time codes for high data rate wireless communication: Performance criteria and code construction," *IEEE Trans. Inform. Theory*, pp. 744-765, Mar 1998.

[5] E. Telatar, "Capacity of multi-antenna Gaussian channels," *AT&T-Bell Laboratories, Internal Tech. Memo*, pp.5-7, June 1995.

[6] S. Alamouti, "A Simple Transmit Diversity Technique for Wireless Communications," *IEEE-JSAC*, Vol.16, No.8, pp. 1451-1458, 1998.

[7] Z. Q. Taha, "Efficient Decoding for Extended Alamouti Space-Time Block code," *International Journal of Distributed and Parallel Systems (IJDPS)*, Vol.2, No.2, pp. 96-103, March 2011.

[8] A. Idris, K. Dimyati, and S. K. Syed Yusof," Performance of Linear Maximum Likelihood Alamouti Decoder with Diversity Techniques," *Proceedings of the World Congress on Engineering*, Vol. 2, July 2011.

[9] C. Min Li, G. Wei Li, and H. Yi Liu," Performance Comparison of the STBC-OFDM Decoders in a Fast Fading Channel, "*Journal of Marine Science and Technology,* Vol.20, No. 5, pp. 534-540.

[10] V. Tarokh, H. Jafarkhani, and A. R. Calderbank, "Space–time block codes from orthogonal designs," *IEEE Trans. Inform. Theory*, Vol.8, pp. 1451–1458, 1998.

[11] V. Tarokh, H. Jafarkhani, and A. R. Calderbank,"The application of orthogonal designs to wireless communication," *in Proc. IEEE Information Theory Workshop, Killarney, Ireland*, pp. 46–47, June 1998.

[12] H. Jafarkhani, "A quasi orthogonal space-time block code," *IEEE Trans. Comm,* Vol. 49, pp. 1-4, Jan 2001.

[13] V. Tarokh, N. Seshadri, and A. R. Calderbank, "Space-time codes for high data rate wireless communication: Performance criteria and code construction," *IEEE Trans. Inform. Theory*, pp. 744 – 765, Mar 1998.

[14] V. Tarokh, A. Naguib, N. Seshadri, and A. R. Calderbank, " Space-Time Codes for High Data Rate Wireless Communication: Mismatch Analysis," *IEEE Trans. Inform. Theory,* Vol.1, pp. 309 – 313, 1997.

[15] V. Tarokh, H. Jafarkhani, and A. R. Calderbank, "Space time block Coding for Wireless Communications: Performance Results," *IEEE Journal on Selected Areas in Communication*, Vol. 17, No. 3, pp. 451–459, July 1999.

[16] Y. Hyun Kimo and J. Young Kim, "Differential STBC MIMO-OFDM System with Cyclic Delay Diversity for Mobile Multimedia Communication Systems," *Kwangwoon University, Seoul, Korea*, pp.1660-1664, Feb 2007.

[17] A. Nagy, G. M. Abdel-Hamid and A.E. Abdalla, "Performance Analysis of DSTBC over VHF Air-to-Ground Communication Channels," *International Journal of Computer Applications (0975 – 8887),* Vol 61– No.9, pp.34-38, January 2013.

[18] S. P. Alex and L. M. A. Jalloul, "Performance Evaluation of MIMO in IEEE802.16e/WiMAX," *IEEE Journal of Selected Topics in Signal Processing,* Vol. 2, pp. 181-190, 2000.

[19] Z. Kan, H. Lin, L. Gang, C. Hanwen, W. Wang and M. Dohler, "Beyond 3G Evolution," *IEEE Vehicular Technology Magazine,* Vol. 3, pp. 30-36, 2008.

[20] A. Himal and S. Suraweera, "Alamouti Coded OFDM in Rayleigh Fast Fading Channels - Receiver Performance Analysis," *IEEE Tencon Conf.* , pp. 1-5, Nov 2005.

[21] W. Chen," Time- Frequency- Selective Channel Estimation of OFDM Systems‘" Drexel University, pp.28-31, October 2005.

[22] Wireless Communication. Retrieved June 15, 2011, from http://www.wirelesscommunication.nl/reference/chaptr05/digimod/awgn.htm.

[23] S. Amjad Ali, "Performance Analysis of Turbo Codes over Fading Channels with Additive White Gaussian and Impulsive Noise," *Eastern Mediterranean University*, pp.12-17, May 2007.

[24] B. Sklar, "Rayleigh Fading Channels in Mobile Digital Communication Systems Part I: Characterization," *IEEE Communications Magazine 35(7): 90-100*. July 1997.

[25] T. S. Rappaport, "Wireless Communications Principles & Practice," *Prentice Hall*، 1996.

[26] H. Hamid and J. Jafarkhani," Space time coding theory and practice," *University of California, Irvine, Cambridge University Press 2005*, pp.7-10.

[27] R. G. Gallager, "Low-Density Parity-Check Codes," Cambridge, MA: MIT Press, 1963.

[28] G. S. Prabhu and P. Mohana Shank, "Simulation of Flat Fading Using MATLAB for Classroom Instruction," *Department of Electrical and Computer Engineering Drexel University, Chestnut Street Philadelphia*, PA 19104 p5.

[29] G. Hill, "Peak Power Reduction in Orthogonal Frequency Division Multiplexing Transmitters, "*Victoria University of Technology School of Communications & Informatics*, March 2011.

[30] A. Cortes, I. Velez, M. Turrillas and J. F. Sevillano," Fast Fourier Transform Processors: Implementing FFT and IFFT Cores for OFDM Communication Systems," *TECNUN (Universidad de Navarra) and CEIT Spain*.

[31] P. Payaswini and D.H. Manjaiah, "Analysis of effect of Cyclic Prefix on Data Rate OFDM Modulation Techniques," *International Journal of Advanced Computer and Mathematical Sciences ISSN 2230-9624*, Vol 3, Issue 4, pp .465-470, 2012.

[32] G.J. Foschini and M. Gans," On limits of wireless communications in fading environment when using multiple antennas," *Wireless Pers. Commun. 6*: 311-335, 1998.

[33] I. E. Telatar,"Capacity of multi antenna Gaussian channels, "*European Trans. Telecommun. 10 (6): 585-59*5, Nov-Dec 1999.

[34] V. Tarokh, and H. Jafarkhani, "A differential detection scheme for transmit diversity," *IEEE Journal on Selected Areas in Communications, 18 (7):* July 2000. 1169–74.

[35] A. G. Dabak, S. Hosur, T.Schmidl and C. Sengupta, "A comparison of the open loop transmit diversity schemes for third generation wireless Systems," No. 1, 2000.

[36] V. Tarokh, H. Jafarkhani and A. Calderbank, " Space–Time Block Coding for Wireless Communications: Performance Results," *IEEE Journal on selected Areas Communications,* Vol. 17, No. 3, pp. 451-459, March 1999.

[37] G. Ganesan, and P. Stoica, "Differential modulation using space-time block code" *IEEE Signal Processing Letters, 9 (2),* pp. 57–60, 2002.

[38] H. Jafarkhani, "Space time coding theory and practice," *Cambridge University Press*, pp. 195-200, 2005.

[39] Wireless OFDM Systems. The University of Texas at Austin from http://www.ece.utexas.edu/~rheath/research

[40] R. John Barry and A. Edward Lee, " Digital Communication," Kluwer Academic Publisher: Third Edition.